Developmental Cell
Article

# Gradients of a Ubiquitin E3 Ligase Inhibitor and a Caspase Inhibitor Determine Differentiation or Death in Spermatids

Yosef Kaplan,[1] Liron Gibbs-Bar,[1] Yossi Kalifa,[1] Yael Feinstein-Rotkopf,[1] and Eli Arama[1,*]
[1]Department of Molecular Genetics, Weizmann Institute of Science, Rehovot, 76100, Israel
*Correspondence: eli.arama@weizmann.ac.il
DOI 10.1016/j.devcel.2010.06.009

## SUMMARY

**Caspases are executioners of apoptosis but also participate in a variety of vital cellular processes. Here, we identified Soti, an inhibitor of the Cullin-3-based E3 ubiquitin ligase complex required for caspase activation during *Drosophila* spermatid terminal differentiation (individualization). We further provide evidence that the giant inhibitor of apoptosis-like protein dBruce is a target for the Cullin-3-based complex, and that Soti competes with dBruce for binding to Klhl10, the E3 substrate recruitment subunit. We then demonstrate that Soti is expressed in a subcellular gradient within spermatids and in turn promotes proper formation of a similar dBruce gradient. Consequently, caspase activation occurs in an inverse graded fashion, such that the regions of the developing spermatid that are the last to individualize experience the lowest levels of activated caspases. These findings elucidate how the spatial regulation of caspase activation can permit caspase-dependent differentiation while preventing full-blown apoptosis.**

## INTRODUCTION

Programmed cell death is one of the most fundamental processes in biology (Raff, 1998; Gilbert, 2001). A morphologically distinct form of this active cellular suicide process, dubbed apoptosis, serves to eliminate unwanted and potentially dangerous cells during development and tissue homeostasis in virtually all multicellular organisms (Jacobson et al., 1997; Tittel and Steller, 2000; Baehrecke, 2002; Yin and Thummel, 2005). Members of the caspase family of proteases are the central executioners of apoptosis. Caspases start off as inactive proenzymes and are activated upon proteolytic cleavage by other caspases (Salvesen and Riedl, 2008). Apoptotic caspases can also participate in a variety of vital cellular processes, including differentiation, signaling, and cellular remodeling (for review, see Kuranaga and Miura, 2007; Yi and Yuan, 2009; Feinstein-Rotkopf and Arama, 2009). However, the mechanisms that protect these cells against excessive caspase activation and undesirable death have remained obscure.

In both insects and mammals, spermatids eliminate their bulk cytoplasmic content as they undergo terminal differentiation. In *Drosophila*, an actin-based individualization complex (IC) slides caudally along a group of 64 interconnected spermatids, promoting their separation from each other and the removal of most of their cytoplasm and organelles into a membrane-bound sack called the cystic bulge (CB), which is eventually discarded as a waste bag (WB) (Tokuyasu et al., 1972; Fabrizio et al., 1998) (see also Figure 2C). This vital process, known as spermatid individualization, is reminiscent of apoptosis and requires apoptotic proteins including active caspases (Arama et al., 2003; Huh et al., 2004; Arama et al., 2006; Muro et al., 2006). However, the mechanisms that restrict caspase activation in spermatids, as opposed to their full-blown activation during apoptosis, are poorly understood.

Recently, we described the isolation of a Cullin-3-based E3 ubiquitin ligase complex required for caspase activation during spermatid individualization (Arama et al., 2007). Ubiquitin E3 ligases tag cellular proteins with ubiquitin, thereby affecting protein localization, interaction, or turnover by the proteasome (Glickman and Ciechanover, 2002; Chen and Sun, 2009). The Cullin-RING ubiquitin ligases (CRLs) comprise the largest class of E3 enzymes, conserved from yeast to human. Cullin family proteins serve as scaffolds for two functional subunits: a catalytic module, composed of a small RING domain protein that recruits the ubiquitin-conjugating E2 enzyme, and an adaptor subunit which binds to the substrate and brings it within proximity to the catalytic module (Petroski and Deshaies, 2005). In Cullin-3-based E3 ligase complexes, BTB-domain proteins interact with Cullin-3 via the eponymous domain, while they bind to substrates through additional protein-protein interaction domains, such as MATH or Kelch domains (Pintard et al., 2004). A large body of evidence indicates that substrate specificity and the time of ubiquitination are determined by posttranslational modifications of the substrates and the large repertoire of the adaptor proteins (Petroski and Deshaies, 2005). In addition, the Cullins themselves are subject to different types of posttranslational regulation. Most notably, they are activated by a covalent attachment of a ubiquitin-like protein Nedd8 (Wu et al., 2006; Bosu and Kipreos, 2008; Merlet et al., 2009).

Here, we identify a small protein called Soti that specifically binds to Klhl10, the adaptor protein of a Cullin-3-based E3 ubiquitin ligase complex required for caspase activation during the nonapoptotic process of spermatid individualization. We show that Soti acts as a pseudosubstrate inhibitor of this E3 complex and that inactivation of Soti leads to elevated levels of

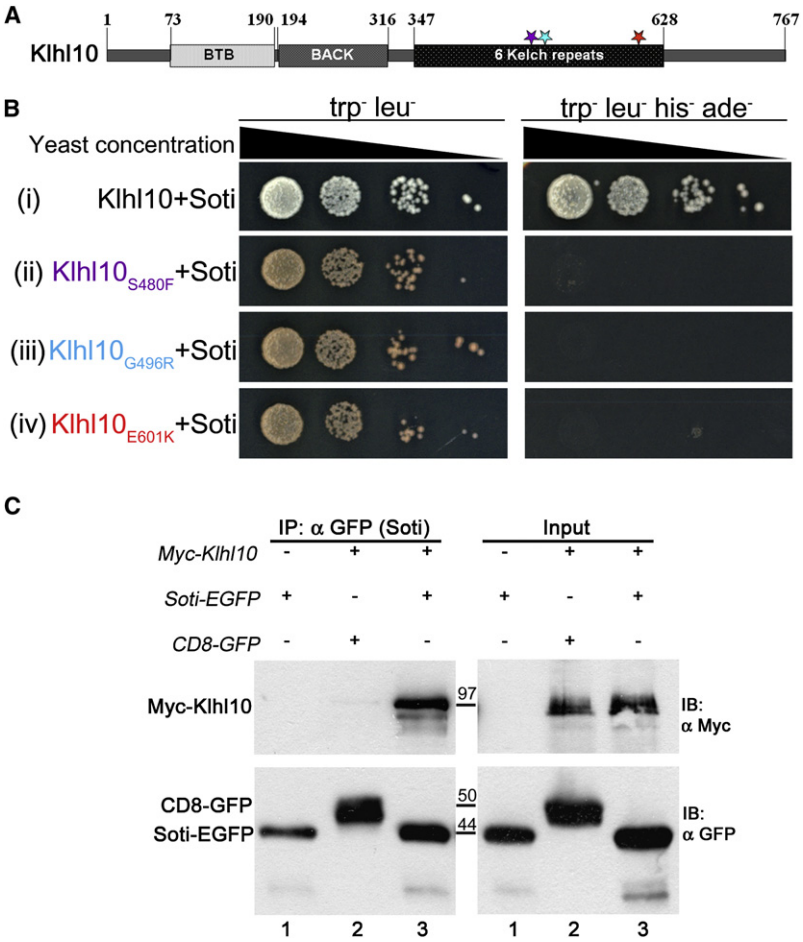


**Figure 1. The Substrate Recruitment Protein Klhl10 Binds to Soti in Yeast and S2 Cells**

(A) Schematic representation of the Klhl10 protein showing the relative locations of the BTB, BACK, and Kelch domains, which are depicted by thick bars. Stars depicting the locations of the different mutations are color-coded to correspond to the colored mutant Klhl10 alleles in (B).

(B) A yeast growth assay on selective media plates was used to assess the interaction of Soti with wild-type or three mutant versions (see also in A) of Klhl10. Yeast colonies which contain both the bait and pray vectors can grow on a medium lacking tryptophan and leucine (−2), while protein-protein interaction events are revealed by the growth on a medium that also lacks histidine and adenine (−4). Four different concentrations of the plated yeast colonies are shown in a descending order from left to right.

(C) S2 cells were cotransfected with Myc-tagged Klhl10 and either Soti-EGFP or CD8-GFP (control) constructs. Anti-GFP Ab was used to immunoprecipitate the Soti complex, while the presence of Klhl10 was detected using anti-Myc Ab. Pre-incubated lysates are shown to the right (Input).

active effector caspases and progressive severity of individualization defects in spermatids. Furthermore, we demonstrate that the giant inhibitor of apoptosis (IAP)-like protein dBruce is targeted by this E3 complex and that this effect is antagonized by Soti. Finally, immunofluorescence studies reveal that Soti is expressed in a distal-to-proximal gradient, which promotes a similar distribution of dBruce in spermatids. Consequently, activation of caspases is restricted in both space and time, displaying a proximal-to-distal complementary gradient at the onset of individualization.

## RESULTS

### The Small Protein Soti Specifically Interacts with Klhl10 in Yeast and S2 Cells

To study the Cullin-3-dependent pathway for caspase activation in spermatids, we conducted a yeast two-hybrid screen to identify potential binding partners for the BTB and Kelch domain-containing protein, Klhl10. Since full-length Klhl10 produces transactivation by itself, a truncated version of this protein (amino acids 188–767) that lacks the BTB domain was used as bait to screen a library of adult *Drosophila* cDNAs (Figure 1A; see also Experimental Procedures). About one-third of the positive cDNA clones correspond to a gene called *scotti* (*soti*; FlyBase gene CG8489), which encodes a small 147 aa protein of unknown function and without any known domains.

Given our previous findings that specific point mutations altering conserved amino acid residues in the Kelch domain of Klhl10 block effector caspase activation and spermatid individualization (Figure 1A) (Arama et al., 2007), we asked whether these mutations may also affect the interaction with Soti. For this, we examined interactions between Soti and three different mutant versions of Klhl10 in yeast. While Klhl10 with an intact Kelch domain readily binds to Soti, as indicated by the yeast growth on selective media, this interaction is completely abrogated by each of the three point mutations (Figure 1B; the colored Klhl10 mutants correspond to the colored stars in Figure 1A). Therefore, Soti may be a physiologically relevant interactor protein of the Klhl10-Cul3 complex.

To further confirm the physical interaction between Klhl10 and Soti, coimmunoprecipitation (co-IP) assays were performed using S2 cells and different expression vectors of these proteins. We found that Klhl10 is present in Soti immunoprecipitates (Figure 1C). Inversely, Soti was coprecipitated with Klhl10 in a reciprocal experiment (see Figure S1A available online). Finally, both Klhl10 and $Cul3_{Testis}$ were coprecipitated with Soti (Figure S1B). We conclude that Soti is a specific interactor of the Klhl10-Cul3 complex.

### *soti* Mutant Spermatids Display Elevated Levels of Active Effector Caspase and Progressive Defects during Spermatid Individualization

To explore the role of Soti in spermatids, we first generated *soti* null mutants by imprecisely excising a *P*{XP} element inserted 468 bp upstream to the *soti* transcriptional start point (Figure 2A). One of the excised lines, $soti^{sik}$, contains a 1393 bp deletion comprising the entire promoter and coding regions of *soti* and

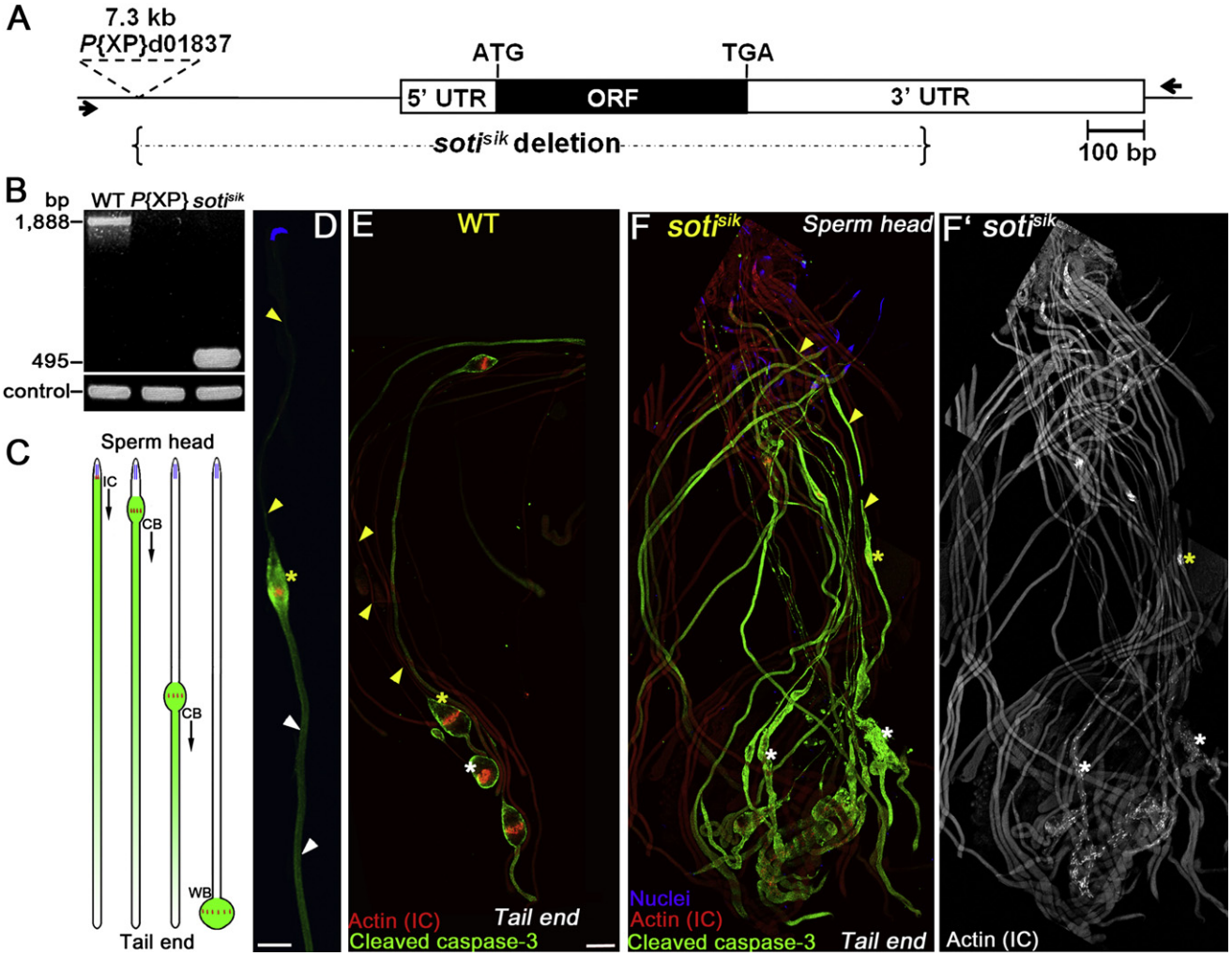


**Figure 2. *soti* Mutant Spermatids Exhibit an Elevated Level of Active Effector Caspase and Progressive Individualization Defects**

(A) A scheme of the genomic organization of the *soti* locus where thick bars indicate the single exon while thin lines represent genomic sequences. Solid and open bars depict coding region (ORF) and UTRs, respectively. The relative location of the *P*-element insertion used for imprecise excision is shown with an inverted triangle. The deleted region in the $soti^{sik}$ allele is flanked by braces.

(B) A genomic PCR experiment for amplifying the *soti* locus from wild-type (WT) and the $soti^{sik}$ mutant flies using the primers that are depicted by arrows in (A). Flies with the original 7.3 kb long *P*{XP} insertion were used for negative control.

(C) Schematic diagram showing four elongated spermatid cysts at increasingly advanced developmental stages (from left to right) during the individualization process. The individualization complex (IC) is in red, nuclei in blue, and active caspases in green. The advancing cystic bulge (CB) collects the spermatids' cytoplasm and most of the organelles and eventually is pinching off from the base of the cyst and discarded as a waste bag (WB).

(D) The proximal region of a single wild-type spermatid cyst during the individualization process stained with anti-cleaved caspase-3 antibody (green), phalloidin which labels the IC, and DAPI to visualize the nuclei (blue). The CB is marked with an asterisk, the postindividualized region of the spermatids is shown with yellow arrowheads, and the preindividualized region is shown with white arrowheads. Scale bar, 25 μm.

(E and F) Elongated spermatids from wild-type (E) and $soti^{sik}$ mutant (F) males were stained with anti-cleaved caspase-3 antibody (green), phalloidin which labels the actin-based investment cones of the IC and also counterstains the spermatids (red), and DAPI to visualize the nuclei (blue; the wild-type image in E does not extend to the nuclear region). The red channel in (F) is also shown in (F′). The spermatid cysts are oriented as in (C). CBs and WBs in wild-type and the corresponding structures in the $soti^{sik}$ mutants are marked with yellow and white asterisks, respectively. Yellow arrowheads are pointing at the postindividualized regions of the spermatids. Scale bar, 50 μm.

thus is a null *soti* allele (Figures 2A and 2B). Flies homozygous for $soti^{sik}$ or in *trans* to a deletion that covers the *soti* locus were viable, female fertile, but male sterile (data not shown).

Our previous genetic data suggest that the normal function of the Cullin-3-based complex in the testis is required for caspase activation and spermatid individualization (Arama et al., 2007). If the interaction of Soti with this complex bears physiological relevance in vivo and Soti indeed serves as substrate or regulator of this complex, we would expect that inactivation of *soti* would cause individualization defects and affect the level of caspase activation in spermatids. To explore this possibility, $soti^{sik}$ mutant testes were dissected and stained to visualize active effector caspases, the individualization complex (IC), and the spermatids' nuclei. Although $soti^{sik-/-}$ spermatids exhibited no gross defects

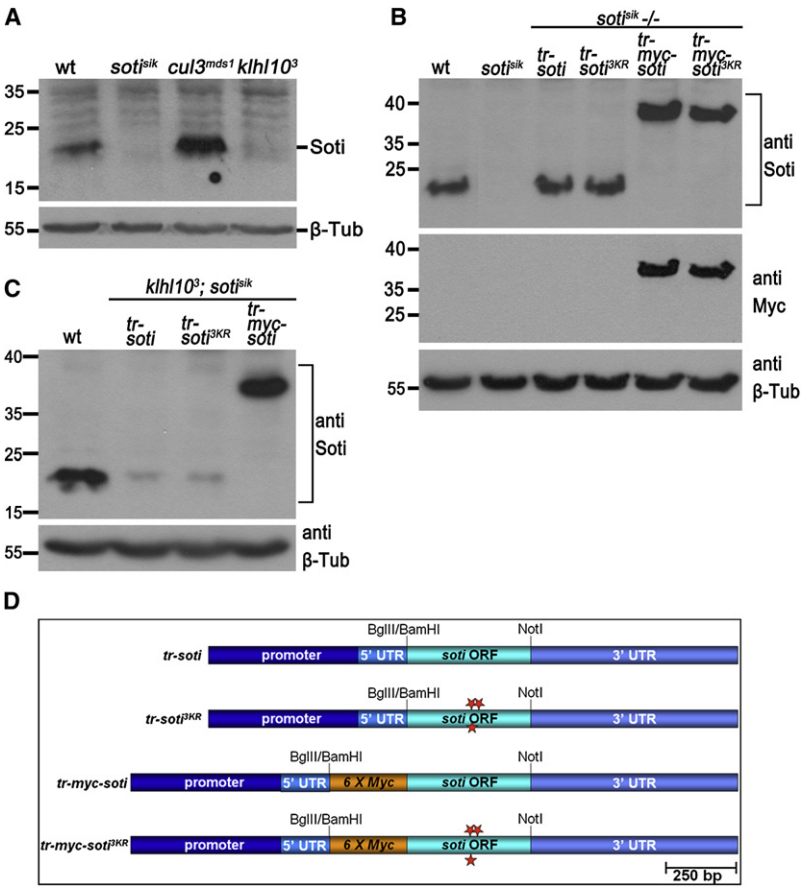


**Figure 3. Klhl10 Is Required for Soti Stabilization**

(A–C) Soti protein levels were assessed by western blotting of protein extracts from dissected testes of the indicated genotypes, using the anti-Soti antibody. β-tubulin protein levels served as loading control. (B–D) Transgenic rescue experiments were performed using the rescue constructs depicted in (D), in the background of either $soti^{sik}$ homozygous mutants (B) or $klhl10^{3}$ and $soti^{sik}$ double homozygous mutants (C). (D) Schematic structures of the rescue constructs for $soti^{sik-/-}$ male sterile flies. All constructs are composed of the *soti* promoter region (dark blue) and 5′ UTR (light blue) that were fused upstream of the coding regions (ORFs) of either *soti* (*tr-soti*), a lysine-less soti (*tr-soti*$^{3KR}$), or N-terminal 6xmyc tagged (orange) *soti* (*tr-myc-soti*) or $soti^{3KR}$ (*tr-myc-soti*$^{3KR}$), followed by the 3′ UTR of *soti* (light blue). The red stars depict the locations of the three lysines that were converted to arginines.

during early and mid stages of spermatogenesis (data not shown), severe defects were observed during spermatid individualization, and as a consequence, mature sperm were not accumulated in the seminal vesicle (data not shown). These mutant spermatids displayed an overall elevated level of active effector caspases when compared with their wild-type counterparts (compare Figures 2E and 2F). Furthermore, whereas the spermatids' cytoplasmic contents (including the active effector caspases) are normally removed from the postindividualized portions of the spermatids into the cystic bulge (Figure 2C and yellow arrowheads in Figures 2D and 2E), in $soti^{sik}$ mutants, cystic bulges were remarkably flat due to a significant amount of cytoplasm which was left behind, in what was supposed to have been the postindividualized region of the spermatids (yellow arrowheads following trails of residual cytoplasm in Figure 2F; asterisks in Figures 2F and 2F′ mark the position of some advanced ICs).

Notably, the advancement of the IC toward the tail end of the spermatids was accompanied by a gradual increase in the severity of the observed individualization defects, such that eventually all the ICs arrested around the final quarter of the spermatids' tails, exhibiting scattered investment cones and failure to generate mature waste bags (arrested ICs are marked by whites asterisks in Figures 2F and 2F′; a wild-type waste bag is denoted by white asterisk in Figure 2E). We conclude that Soti functions to inhibit caspase activation in spermatids and that its action is crucial for the proper removal of the spermatids' cellular contents during the process of individualization.

## Soti Is Not a Target for Proteolysis by the Klhl10-Cul3 Ubiquitin Ligase Complex

We next investigated whether Soti is targeted for ubiquitination-mediated degradation by the Klhl10-Cul3 complex by assessing the level of the Soti protein in mutants of this complex. For this, a specific polyclonal antibody was raised against full-length Soti and its specificity was tested by western blot analysis. A 17 kDa band of Soti was detected in wild-type but not in testis extracts from $soti^{sik-/-}$ flies, confirming the specificity of this antibody (Figure 3A). Unexpectedly, however, although about a 2.5-fold increase in the level of Soti was observed in the *cullin-3* mutant ($cul3^{mds1}$), Soti was nearly absent from the *klhl10* mutant testes (Figure 3A). Similar observations were made using whole-mount immunofluorescence staining of mutant testes (Figures S2A–S2D). Furthermore, when cotransfected into S2 cells, Soti was less stable in the absence of Klhl10 (Figure S1A, compare lane 2 marked with an asterisk and lanes 3 and 4 in the anti-Soti blot in the ''Input''). Therefore, not only is Soti not a target for proteolytic degradation by the Klhl10-Cul3 complex, but in fact, Soti is stabilized in the presence of Klhl10.

## Soti Is Degraded by a Noncanonical Pathway during Spermatogenesis

The fact that Soti protein level is elevated in the *cullin*-3 mutant spermatids suggests that Soti levels are regulated by either a direct or an indirect Cullin-3-dependent mechanism during normal spermatogenesis. We investigated these possibilities by substituting the expression of the endogenous *soti* with transgenic expression of nonubiquitinatable counterparts, which were inserted at a defined site of the *Drosophila* genome (Figure 3D; Experimental Procedures). To block the canonical ubiquitination pathway which occurs on internal lysine residues (Glickman and Ciechanover, 2002), a lysine-less form of Soti

was generated where all the three lysine residues were converted to arginines (*tr-soti*$^{3KR}$; Figure 3D). We also generated two additional forms of Soti that contain 6xMyc tags fused to the N termini of wild-type or lysine-less Soti (*tr-myc-soti* and *tr-myc-soti*$^{3KR}$, respectively), in order to attenuate noncanonical degradation pathways, such as N-terminal ubiquitination or degradation "by default" (Breitschopf et al., 1998; Bloom et al., 2003; Asher et al., 2006).

Each transgenic line was crossed to *soti*$^{sik}$ flies and the ability to express similar protein levels as that of the endogenous Soti and to rescue the male sterility phenotype was tested and confirmed for all of these transgenes (compare *tr-soti* with wild-type [yw] in Figure 3B; Figures S2E–S2H). To our surprise, the level of the lysine-less form of Soti was indistinguishable from that of the intact transgenic form (Figure 3B). In contrast, an approximate 2.5-fold increase above the level of the intact transgenic form was detected with the Myc-tagged forms of Soti, indicating that Soti is normally targeted for degradation by a noncanonical pathway (Figure 3B). Likewise, when *soti* and *klhl10* were both inactive, the intact and lysine-less forms of Soti were almost completely degraded, while the Myc-tagged Soti was markedly stable (Figure 3C; also compare with Figure 3B). We conclude that normal degradation of Soti during spermatogenesis is mediated by a noncanonical pathway stimulated by the release of Soti from Klhl10.

It is well established that adaptor proteins are often unstable and undergo proteasome-mediated degradation as a result of autoubiquitination when linked to the CRL complex (for review, see Bosu and Kipreos, 2008). Therefore, the observed elevation in the level of Soti in *cullin-3* mutant spermatids (Figure 3A) may be attributed to a reduction in autoubiquitination and degradation of Klhl10 in this mutant, which in turn binds to and further stabilizes Soti. To test this possibility, a ubiquitination assay was performed in S2 cells using an HA-tagged Klhl10 and components of the Cullin-3-based complex, Cul3$_{Testis}$ (Arama et al., 2007) and the somatic RING-domain protein Roc1a (Donaldson et al., 2004) (Figure S2I). Low level of HA-Klhl10 ubiquitination was already detected even without cotransfection of additional components of the Cullin-3-based complex (lane 2). This ubiquitination is due to the presence of endogenous Cullin-3, since coexpression of a dominant-negative mutant form of Cul3$_{Testis}$, which lacks the CHD domain and hence cannot bind to the RING protein, markedly attenuated this effect (lane 6). Cotransfection of wild-type Cul3$_{Testis}$ and Roc1a resulted in even stronger HA-Klhl10 autoubiquitination (lane 4), which was not affected by the coexpression of Soti (lanes 3 and 5). Collectively, these results suggest that Klhl10 is normally autoubiquitinated and that Soti does not interfere with this activity.

## Soti Acts Upstream of, and Genetically Interacts with, the Cullin-3-Based Ubiquitin Ligase Complex in Spermatids

Our findings that Soti can physically interact with the Cullin-3-based complex and that inactivation of these genes results in essentially opposing phenotypes (e.g., elevation versus abrogation of caspase activation, respectively) suggest that these components may function in a common pathway but in an antagonistic mode of action. To investigate the mechanistic relationship between Soti and this E3 complex, we first performed genetic epistasis experiments to determine which of the mutant phenotypes prevails in the *soti*$^{sik}$ and the null *cul3*$^{mds1}$ or *klhl10*$^{3}$ double mutant spermatids. Testes from the homozygous double mutants or the different heterozygous combinations of sibling controls were stained to reveal cleaved effector caspase expression during spermatid individualization. As expected, double heterozygous sibling controls exhibited normal caspase activation and spermatid individualization (Figures 4A and 4E), and flies carrying both one homozygous and one heterozygous allelic combinations displayed phenotypic characteristics of the single homozygous counterparts (Figures 4B, 4F, 4C, and 4G). However, in the double homozygous mutants, caspase activation and initiation of individualization were completely abolished. Since these phenotypes are reminiscent of the Cullin-3-based complex mutants, we conclude that Soti acts upstream of the Cullin-3-based complex in spermatids (Figures 4D and 4H).

Next, we tested the idea that Soti may function to antagonize the activity of this E3 complex and asked whether inactivation of Soti can compensate, at least in part, for the loss of the Cullin-3 activity. For this, we took advantage of the availability of several weak (hypomorphic) *cullin-3* mutants, which fail to initiate individualization but still exhibit a low level of caspase activation (Arama et al., 2007). These mutants were used to test for genetic interaction between *soti* and *cullin-3*, by generating double mutant flies. As before, testes were stained to visualize the individualizing spermatids, and the sibling controls exhibited the expected phenotypes (Figures 4I and 4J). Interestingly, whereas homozygous double mutants were still infertile, some highly reduced translocating ICs were frequently detected (arrows in Figure 4L). These ICs were never observed in *cul3*$^{mds5}$ homozygous mutants alone or combined with a single *soti*$^{sik}$ allele (Figure 4K). These results indicate that in addition to their physical interaction, Soti also antagonizes the activity of the Cullin-3-based complex in spermatids.

## Soti Acts as an Inhibitor of the Cullin-3-Based Ubiquitin Ligase Complex

To test the idea that Soti is an inhibitor of the Cullin-3-based complex, we turned to an in vivo transgenic system; the compound eye of the adult *Drosophila*. The eye-specific *GMR-GAL4* line was used to drive expression of the *UAS*-dependent transgenes. Whereas transgenic expression of the cytotoxically inert green fluorescent protein (GFP) did not cause any gross eye defect, a highly reduced eye size with disorganized ommatidial array was induced following expression of a single copy of a *klhl10* transgene (Figures 4M and 4N). In contrast, no effect on eye morphology was detected when a *klhl10* transgene with a point mutation in the Kelch domain was expressed (Figure 4O). An identical mutation can abrogate effector caspase activation in spermatids (Arama et al., 2007) and the interaction with Soti (Figures 1A and 1B). Thus, transgenic Klhl10 exerts its activity in a similar mode as that of endogenous Klhl10, albeit it may engage different substrates. Significantly, transgenic expression of a single copy of *soti*, which by itself did not cause any abnormal morphology, completely suppressed the *klhl10*-dependent eye phenotype, demonstrating that Soti is a potent inhibitor of Klhl10 (Figures 4P and 4Q).

Further analysis of this eye system revealed that the effect of transgenic *klhl10* can be markedly enhanced by transgenic expression of *cul3*$_{Testis}$ and that Soti can completely suppress

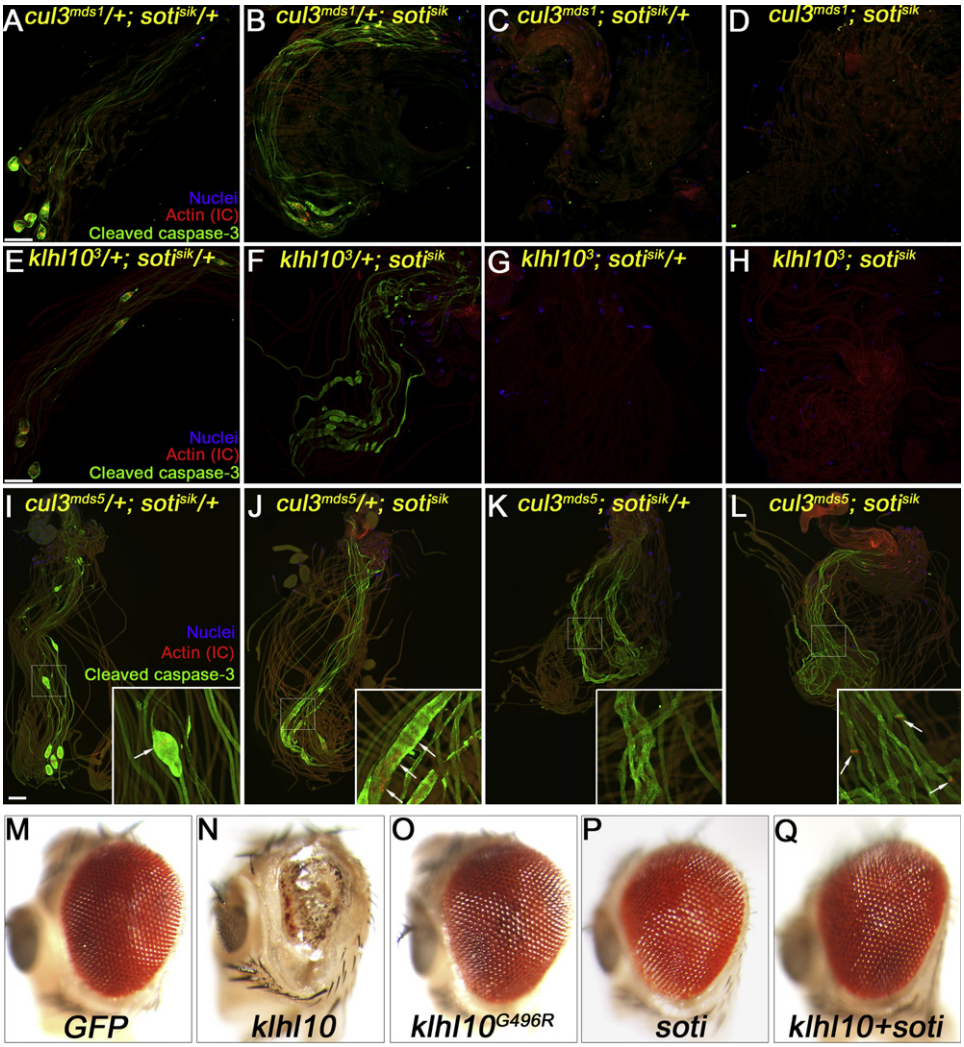


**Figure 4. Soti Is an Inhibitor of the Cullin-3-Based Ubiquitin Ligase Complex**

(A–L) Epistasis experiments between Soti and the components of the Cullin-3-Klhl10 complex. In these experiments, $soti^{sik}$ mutant flies were crossed to the following fly lines: (A–D) a null allele of $cul3_{Testis}$ ($cul3^{mds1}$), (E–H) a strong loss-of-function mutation in *klhl10* ($klhl10^{3}$), and (I–L) a hypomorphic allele of $cul3_{Testis}$ ($cul3^{mds5}$), which still displays some level of active effector caspase expression. Testes were stained as in Figure 2. Scale bars for (A–H) and (I–L), 100 μm. (M–Q) Transgenesis experiments using the *Drosophila* adult compound eye. The UAS-dependent transgenes, indicated below each panel, were ectopically expressed in the eye imaginal discs, using two copies of the *GMR-GAL4*. Representative eyes from newly eclosed females are shown.

this strong phenotype (Figures S3A–S3E and Figures S3A′–S3E′). This synergistic effect requires the assembly of an active Cullin-3-based complex, as transgenic expression of a catalytically inactive $cul3_{Testis}$ failed to enhance the *klhl10* phenotype (Figures S3F–S3H). Finally, using mutant lines heterozygous for either $cul3_{Soma}$ ($cul3^{gft06430}$) or $cul3_{Testis}$ ($cul3^{mds1}$), we demonstrated that most, if not all, of the activity of the transgenic Klhl10 in the eye depends on the presence of an endogenous somatic Cullin-3 isoform (Figures S3I–S3M). Therefore, the ability of Soti to inhibit the action of Klhl10 is exclusively related to the function of Klhl10 in a complex with Cullin-3.

## Soti and Active Caspases Display Opposing Gradients

Caspase activation at the onset of spermatid individualization does not occur uniformly through spermatids. Instead, we observed a graded pattern of active caspase expression descending from sperm heads (nuclear or proximal region) to tail ends (distal region) of spermatids (Figures 5A and 5A′). In the *Drosophila* testis, the developing spermatidal cysts are organized in a circular manner, such that younger cysts are found along the circumference, while more developmentally advanced cysts are located in the middle of the testis (see Figure 2 in Tokuyasu et al., 1972). To determine whether graded activation of caspases is a "normal" phenomenon, which accompanies every spermatidal cyst at the onset of individualization, cross sections of adult testes were stained to visualize active effector caspases and polyglycylated tubulin, a posttranslational modification which occurs on the spermatid tail axoneme at the onset of individualization and persists in mature spermatozoa (Arama et al., 2007; Rogowski et al., 2009). Indeed, early individualizing

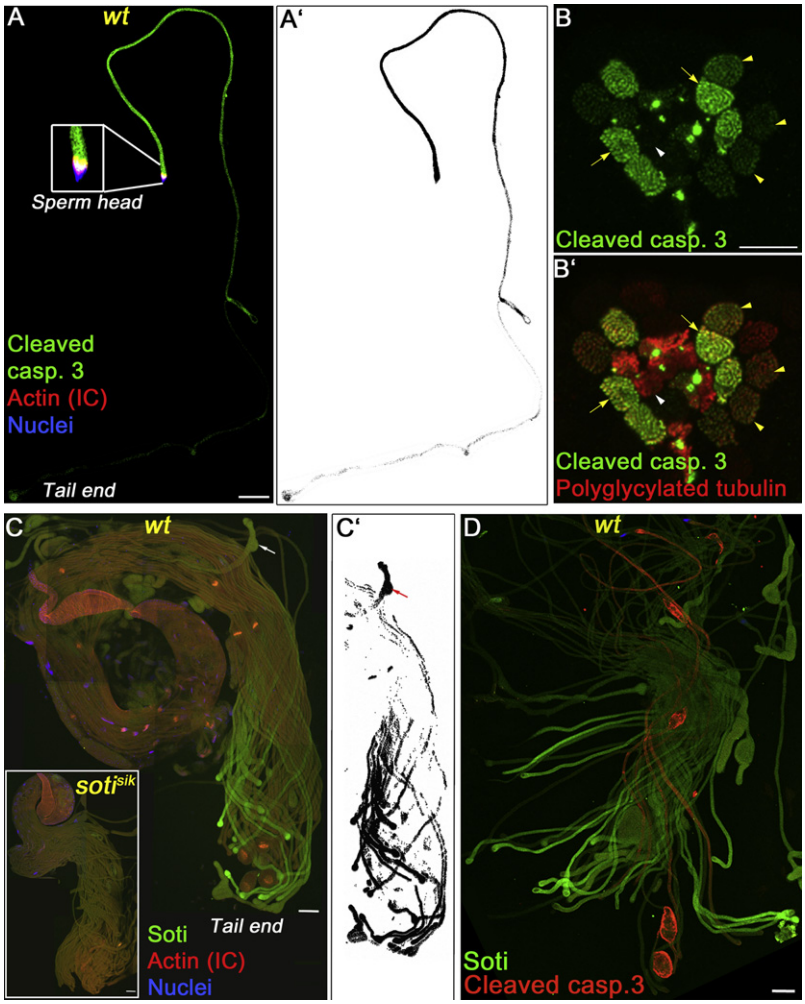


**Figure 5. Opposing Gradients of Soti and Active Effector Caspases in Spermatids**

(A) A wild-type spermatid cyst at the onset of individualization is stained as in Figure 2. The cyst is oriented with the tail end down. Enlargement of the sperm head region which contains the spermatids' nuclei (blue) and the recently assembled IC (red, white, or yellow) is shown in the inset.

(A′) the image in (A) was "grayscaled" and "inverted" using Photoshop to facilitate better visualization of the active effector caspase gradient. Scale bar, 50 μm.

(B and B′) Cross sections of adult testes were stained with anti-cleaved caspase-3 antibody (green) and the AXO49 antibody, which visualizes polyglycylation of axonemal tubulin, a modification that occurs in parallel to caspase activation (red). (B) is the green channel only of (B′). Scale bar, 10 μm.

(C) Visualization of the Soti protein in spermatids using anti-Soti antibody (green). ICs (red) and nuclei (blue) are also visualized. The white or red arrows are pointing at one early elongating spermatid cyst. The inset shows a $soti^{sik-/-}$ testis.

(C′) The image in (C) was modified as in (A′). Scale bars, 50 μm.

(D) The gradient of Soti (green) is detected in wild-type elongating spermatids. Individualizing spermatids are stained red for active effector caspases. Scale bar, 50 μm.

spermatids exhibited low levels of active effector caspase, while more developmentally advanced individualizing spermatids displayed higher levels of active caspases (yellow arrowheads and arrows, respectively, in Figures 5B and 5B′). Cysts with mature spermatozoa were free of active effector caspases, but still displayed polyglycylation (white arrowhead in Figures 5B and 5B′).

The finding that $soti^{sik-/-}$ spermatids display progressive defects during individualization prompted us to explore the spatial distribution of Soti, and whether it has some implications on the pattern of caspase activation. Strikingly, inspection of Soti expression using the affinity-purified anti-Soti antibody on wild-type testes revealed a specific gradient of the Soti protein in elongating spermatids descending from the tail ends to the sperm heads, the opposite direction as that of caspase activation (Figures 5C and 5C′; the inset in Figure 5C shows a lack of staining in the $soti^{sik}$ mutant spermatids control). This gradient likely has a transcriptional origin, as *soti* transcripts were detected at a very low level in premeiotic primary spermatocytes, while in postmeiotic spermatids the signal of *soti* significantly intensified and was restricted to the distal (tail) ends of elongating spermatids, trailing away proximally (asterisk and arrows, respectively, in Figures S4A and S4B) (see also Barreau et al., 2008). Collectively, these results strongly suggest that an inhibitory gradient of Soti may promote the graded activation of caspases in the opposite direction.

## The Klhl10-Cul3 Complex Can Target Large dBruce Polypeptides and Is Antagonized by Soti

Our genetic data indicate that Soti function is required during the process of individualization. However, at the onset of individualization the level of Soti protein already decreases sharply, such that Soti is no longer detected when this process advances (note the absence of Soti in individualizing spermatids marked by active effector caspase staining and the presence of cystic bulges in Figure 5D). Furthermore, the gradient of caspase activation is clearly detected at the onset of individualization, a time when Soti level rapidly decreases (the assembly of an IC marks the onset of individualization as shown in Figure 5A). These observations raise the possibility that Soti-mediated inhibition of the Cullin-3-based complex may promote proper distribution of yet another (caspase) inhibitor, which may persist throughout the process of individualization.

The best-characterized family of endogenous caspase inhibitors are the inhibitor of apoptosis (IAP) proteins (Goyal, 2001; Bergmann et al., 2003). Several lines of evidence suggest that the giant member of this family Bruce/Apollon (Bartke et al., 2004; Hao et al., 2004) is at least one of the substrates for the Cullin-3-based complex in spermatids. Most notably, inactivation of *Drosophila* Bruce (dBruce) causes male sterility due to individualization defects reminiscent of *soti* mutants (Arama et al., 2003) (see also Figures S5A–S5C). Moreover, truncated forms of

dBruce, dBruce "BIR" and dBruce "mini-gene" polypeptides, can bind to the substrate recruitment protein Klhl10 in *Drosophila* S2 cells (Figure 6A; Figure S1A) (see also Arama et al., 2007).

To investigate whether the Cullin-3-based complex can target dBruce, ubiquitination assays were performed in S2 cells. Due to its large size, a full-length cDNA clone of *dbruce* is unavailable, and we thus used two truncated forms of dBruce polypeptides (Figure 6A). Both the smaller ("BIR", 387 aa) and the larger ("mini-gene", 2068 aa) dBruce polypeptides were highly unstable following transfection due to background ubiquitination, but some stability was achieved upon incubation with the proteasome inhibitor MG132 (Figure 6B, lanes 3 and 2, and Figure 6C, lanes 2 and 3, respectively). In the presence of MG132, cotransfection with Klhl10 alone or together with other components of the Cullin-3-based complex ($Cul3_{Testis}$ and Roc1a) further destabilized the dBruce mini-gene over the level with MG132, but not the dBruce BIR polypeptide (Figure 6B, lanes 4 and 5 in the "IP", and Figure 6C, lanes 4 and 6 in both the "'Input" and "IP", respectively). Significantly, both polypeptides were highly stabilized when in addition to the components of the Cullin-3-based complex, cells were also cotransfected with Soti, indicating that Soti strongly antagonizes Klhl10-Cullin-3-mediated regulation of dBruce (Figure 6B, lane 6, and Figure 6C, lanes 5 and 7, respectively). It is noteworthy that cotransfection of catalytically inactive Klhl10 and Cullin-3 mutants also resulted in marked stabilization of the dBruce BIR polypeptide, indicating the higher affinity of this polypeptide to the inactive complex, as opposed to its more transient interaction with the active complex (Figure 6B, lanes 7 and 8). This is consistent with the notion that dBruce BIR polypeptide is also targeted by the Cullin-3-based complex. In conclusion, the Cullin-3-based complex has the potential to target dBruce and this activity is strongly antagonized by Soti.

The interaction of the dBruce mini-gene with Klhl10 was also demonstrated in the *Drosophila* eye system. Transgenic expression of dBruce mini-gene suppressed the rough and small eye phenotype induced by transgenic expression of the pro-apoptotic gene *reaper* (*rpr*) (Figures S3N and S3O). In contrast, similar expression of the dBruce mini-gene dramatically enhanced the small eye phenotype caused by transgenic expression of Klhl10 (Figures S3P–S3S). These results indirectly suggest that in this system, the Cul3-Klhl10 complex does not target the dBruce mini-gene for degradation, but rather leads to an unknown change in the status of this polypeptide, which in turn causes further stress to the cells in the eye.

## Soti and the Giant IAP-Like Protein dBruce Compete for Binding to Klhl10

Since Soti inhibits the Klhl10-Cul3 complex activity by binding to Klhl10, we hypothesized that Soti and dBruce may compete for binding to Klhl10. Indeed, cotransfection of dBruce BIR resulted in 3.5-fold decrease in the level of Soti found in Klhl10 immunoprecipitates, suggesting that some competition may exist (Figure S1A, lanes 3 and 4 in the IP and the quantification in the graph). However, we could also detect the formation of a Soti-Klhl10-dBruce BIR tertiary complex in Soti immunoprecipitates, suggesting that dBruce BIR is not an efficient competitor of Soti (Figure 6D). To examine whether this partial competition effect is due to the relatively small size of dBruce BIR, we repeated the co-IP experiment, but in this case used the five times larger dBruce mini-gene polypeptide. Indeed, no dBruce mini-gene could be coprecipitated with Soti in the presence of Klhl10 (Figure 6E). We conclude that dBruce can compete with Soti for binding to Klhl10.

Our data do not support the idea that neddylation of Cullin-3 may trigger the switch from Soti-bound to dBruce-bound Klhl10-Cul3 complex, since Soti can also interact with the nonneddylated form (Figure S1B, lane 4, lower band), as well as a catalytically inactive Cullin-3 mutant which lacks the CHD domain that also includes the conserved neddylatable lysine residue (Figure S1B, lane 5).

## dBruce Is Distributed in a Gradient of the Same Direction as that of Soti

To examine whether the spatial distribution of the dBruce protein may also have implications on the distribution of active caspases, wild-type testis preparations were stained with anti-dBruce antibody (for antibody properties, see Figure S5F–S5M and Experimental Procedures). Importantly, dBruce is distributed in a gradient of the same direction as that of Soti in spermatids (Figure 7A). Triple staining for dBruce, Soti, and polyglycylated tubulin revealed that in early, mid, and advanced spermatid elongation stages, only the gradient of Soti is visible (developmental stages i and ii, which are also indicated by white arrowheads in Figure 7A, and correspond to the diagram in Figure 7B). dBruce protein starts to accumulate in tail ends prior to the onset of individualization, at a time when the signal of the gradient of Soti is declining (stage iii in Figure 7B; yellow arrowheads in Figures S5D and S5E). Immediately prior to individualization, the signal of dBruce intensifies, while Soti is almost completely absent (late stage iii indicated by yellow arrows in Figure 7A and the scheme in 7B). The dBruce gradient then persists throughout individualization (stage iv; note the presence of dBruce [white arrows]- within spermatids with polyglycylated axonemal tubulin in Figures 7A and 7B). Eventually, when the individualization process terminates, dBruce is removed from spermatids into the waste bag (stage v; a yellow arrowhead in Figure 7A and the scheme in Figure 7B; the waste bag is marked by an asterisk).

## Cullin-3, Klhl10, and Soti Are Required for Proper Distribution of dBruce in Individualizing Spermatids

As opposed to the gradient of Soti, the basis for dBruce distribution is not transcriptional, as determined by RNA in situ hybridization analysis (Figures S4D and S4E). We therefore asked whether the protein distribution of dBruce requires the function of the Cullin-3-based complex. For this, testes from *cullin-3* and *klhl10* homozygous mutants were stained with the anti-dBruce antibody. No dBruce gradient was detected in elongated spermatids from these mutants (compare Figure 7C with Figures 7D and 7E). Instead, a very weak signal of dBruce was detected in tail ends and most of the protein was more uniformly distributed throughout elongated spermatids (Figures 7D and 7E).

To control for a possible indirect effect of the *cullin-3* and *klhl10* mutants on spermatid individualization process, we also stained testes from flies with a mutation in the unconventional myosin VI ($jar^1$), which is required for proper individualization process (Hicks et al., 1999). The dBruce gradient was readily detected in these mutant spermatids, indicating that dBruce

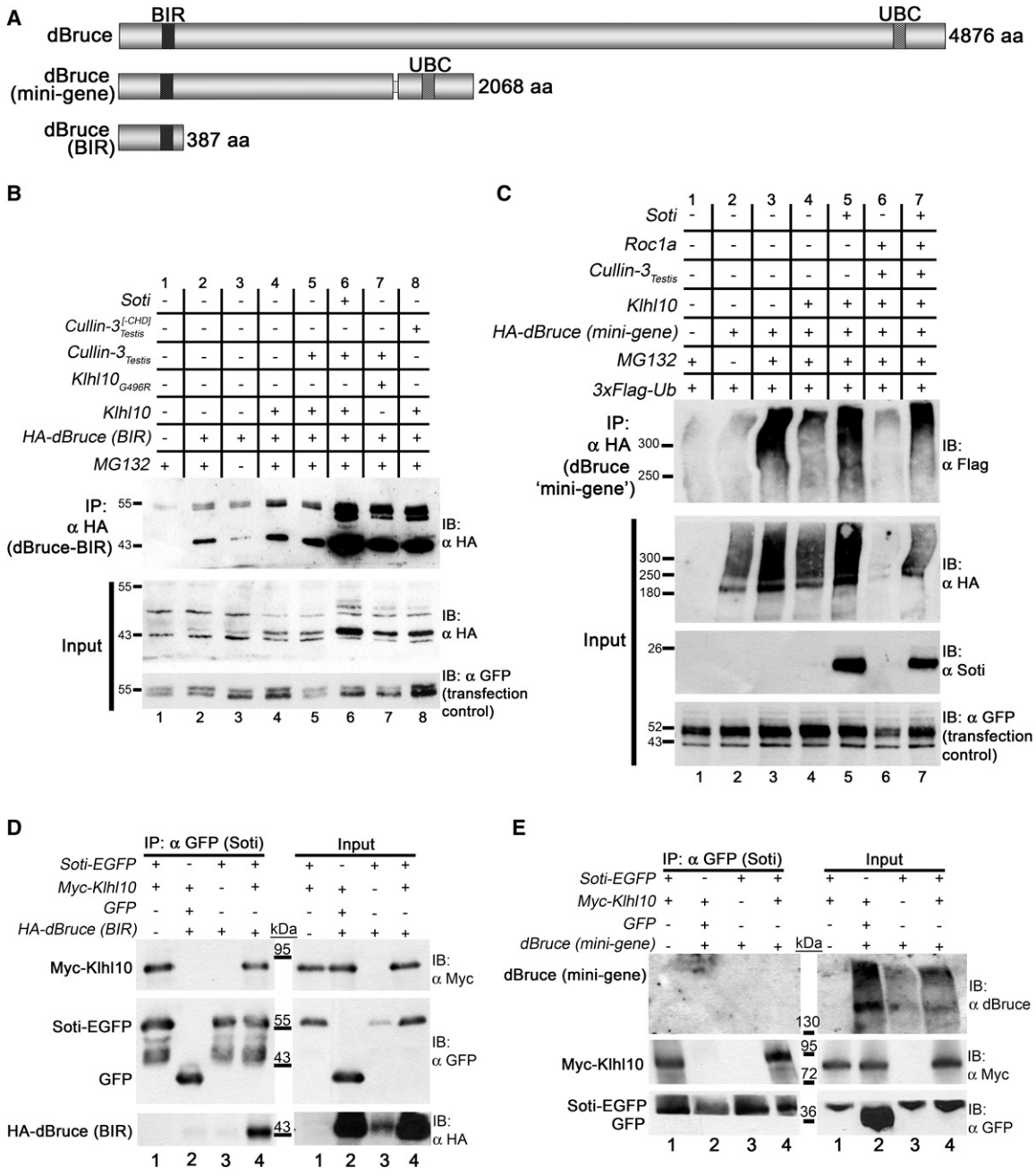


**Figure 6. Biochemical Interactions among the Klhl10-Cul3 Complex, dBruce, and Soti**

(A) Schematic representations of the full-length dBruce protein and the dBruce derivatives (mini-gene and BIR) used in this study. The relative locations of the BIR and UBC domains are depicted by vertical rectangles. The sizes of the different diagrams are to scale and indicated at the right side of each scheme. The dBruce mini-gene consists of the first N-terminal 1622 aa, including the BIR domain, and the last C-terminal 446 aa that contain the UBC domain. The dBruce BIR polypeptide contains the first N-terminal 387 aa of dBruce that include the BIR domain region (amino acids 251–321).

(B) Ubiquitination experiment in S2 cells using the dBruce BIR polypeptide. Cells were cotransfected with HA-tagged dBruce BIR polypeptide and one or more of the following: Klhl10, $Klhl10_{G496R}$ (an inactive Klhl10 mutant which was originally identified in a genetic screen for mutants that failed to activate caspases in spermatids; Arama et al., 2007), $Cul3_{Testis}$, $Cul3_{Testis}^{[-CHD]}$ (a catalytically inactive $Cul3_{Testis}$ which lacks the C-terminal cullin-homology-domain [CHD]), and Soti. In addition, cells were also cotransfected with CD8-GFP (loading and transfection efficiency control) and at 40 hr posttransfection the indicated cells were incubated with the proteasome inhibitor MG132 for 6 hr. Cells were lysed under denaturing conditions and ubiquitinated dBruce BIR polypeptides were isolated with anti-HA beads. The presence of dBruce BIR and its ubiquitinated forms was identified by immunoblotting with the anti-HA Ab.

(C) Ubiquitination experiment in S2 cells using the dBruce mini-gene polypeptide. Cells were cotransfected with HA-tagged dBruce mini-gene polypeptide and one or more of the following: Klhl10, $Cul3_{Testis}$, Roc1a, and Soti. All cells were also cotransfected with Flag-tagged *Drosophila* ubiquitin and CD8-GFP for transfection control and treated as in (B). The presence of dBruce mini-gene or its ubiquitinated forms was identified by immunoblotting with the anti-HA or anti-Flag Abs, respectively.

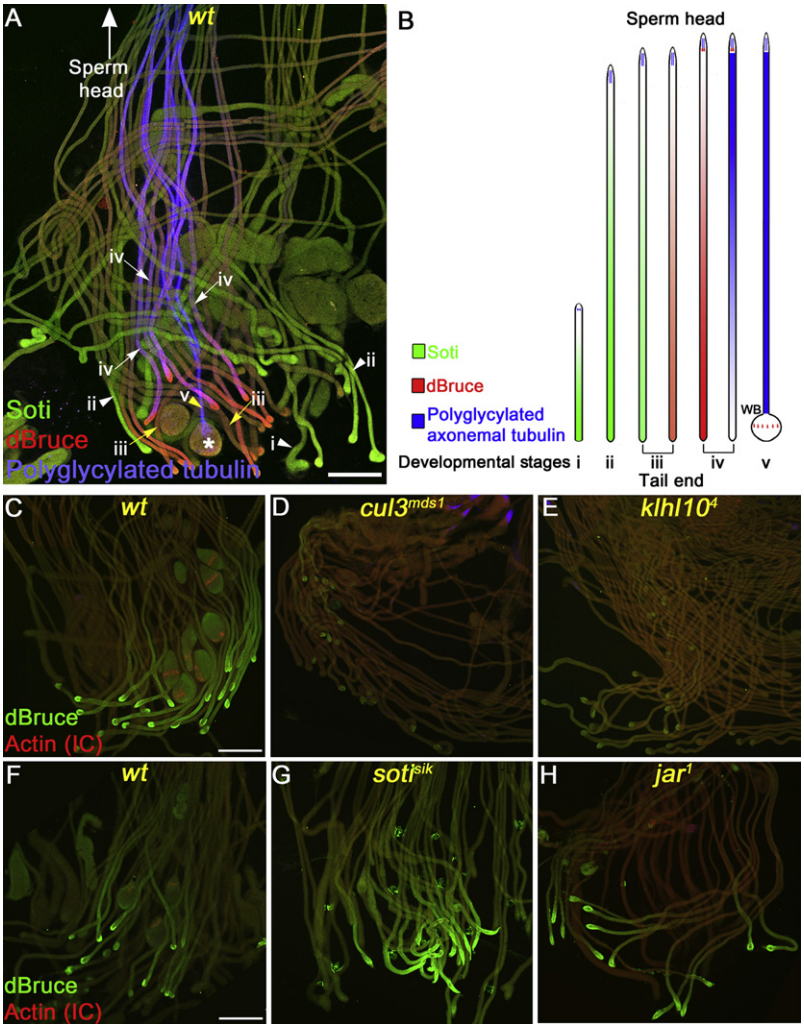


**Figure 7. dBruce Is Distributed in a Gradient that Requires Functional Cullin-3, Klhl10, and Soti**

(A) Wild-type spermatid cysts stained to visualize dBruce (red), Soti (green), and polyglycylated axonemal tubulin (blue), a marker for the individualization stage.

(B) Schematic representation of the different developmental stages and stainings of the spermatid cysts that are indicated in (A). In (A) and (B), the roman numerals depict different developmental stages and are accompanied by different arrows or arrowheads in (A). The asterisk marks a waste bag. Scale bar, 100 μm.

(C–H) Testes from wild-type (wt) and the indicated mutant flies were stained to visualize dBruce (green). ICs are in red. Scale bars, 100 μm.

distribution is independent of other aspects of spermatid individualization (Figure 7H). We then investigated whether the function of Soti as an inhibitor of the Cullin-3-based complex is linked to the proper distribution of dBruce in spermatids. In *soti* mutants, dBruce protein was remarkably more concentrated at tail ends of spermatids than in wild-type (compare Figure 7F with Figure 7G). Since this effect is essentially opposite to that of the mutants for the Cullin-3-based complex, we conclude that the balanced actions of Soti and the Cullin-3-based complex are essential for the proper redistribution of dBruce in spermatids.

## DISCUSSION

### An Integrated Model for the Function of the Ubiquitin Pathway during Late Spermatogenesis

The current study provides insight into how some cells can utilize active caspases to promote vital cellular processes but still avoid unwanted death. According to this model (Figure 8), during early and advanced spermatid developmental stages, a gradient of Soti is generated, allowing graded activation of the Cullin-3-based E3 ubiquitin ligase complex in the opposite direction. This E3 complex then targets dBruce, promoting its distribution in a similar gradient as that of Soti. Subsequently, caspase activation occurs in a complementary gradient descending from proximal to distal. Since the removal of the cytoplasm and caspases also occurs in the direction of proximal to distal, the regions of the developing spermatid that are the last to individualize are also those that are the most protected against activated caspases. This setting ensures that each spermatidal domain encounters similar transient levels of activated caspases throughout the process of individualization.

The gradual regulation of caspase activity in spermatids is attributed to the outstanding length of *Drosophila* spermatids (a phenomenon called sperm gigantism). Spermatozoa of *Drosophila melanogaster* are about 1.9 mm long and other *Drosophilids* can produce sperm up to 58 mm long (Pitnick et al., 1995). Spermatids in *D. melanogaster* individualize over the course of 12 hr through a constant rate of proximal-to-distal individualization complex movement and clearance of the cytoplasmic content (including the active caspases) into a cystic bulge (Noguchi and Miller, 2003). Since it takes a few hours for the active effector caspases to kill a cell (Morgan and Thorburn, 2001), spermatids had to develop an efficient mechanism to prevent prolonged exposure of the more distal cellular regions to caspase activity. A gradient of a caspase inhibitor, descending from distal to proximal, is therefore an elegant mechanism to ensure a level of caspase activity that is sufficient to drive spermatid differentiation, yet not high enough to engage an apoptotic program.

(D and E) Co-IP assays with Soti and either the dBruce BIR polypeptide or mini-gene in the presence or absence of Klhl10. S2 cells were cotransfected with EGFP-tagged Soti (or EGFP alone as control), Myc-tagged Klhl10, and either an HA-tagged dBruce BIR polypeptide (D) or a nontagged dBruce mini-gene (E). The EGFP immunoprecipitates (IP) and the corresponding preincubated lysates (Input) were analyzed by immunoblotting (IB) with the indicated antibodies.

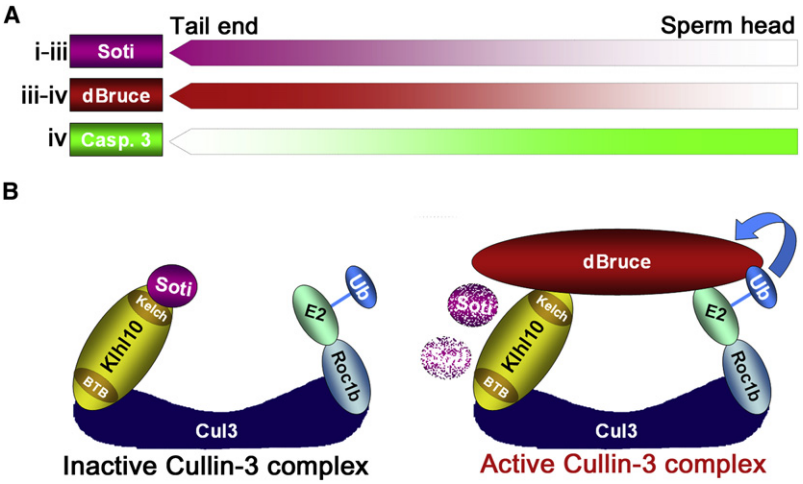


**Figure 8. A Model of Spatial Restriction of Caspase Activation**

(A) Diagrams of the relative gradients of Soti (purple), dBruce (red), and active effector caspase (green; Casp. 3) in spermatids. The temporal expression patterns are depicted by roman numerals, which correspond to the different developmental stages in Figure 7B.

(B) The inactive and active states of the Cullin-3-based ubiquitin ligase complex coexist in the same individualizing spermatid due to the graded expression of its inhibitor Soti. Just prior to the onset of individualization, dBruce begins to accumulate, binds to the Cullin-3-Klhl10 complex, from which Soti is displaced and subsequently degraded by a noncanonical pathway. dBruce ubiquitination contributes to the formation of an appropriate gradient at the onset of individualization. Caspases are then activated in a complementary gradient.

## How Does Ubiquitination of dBruce Promote Its Graded Distribution?

Ubiquitination may target dBruce for either degradation or active redistribution. Because of technical limitations of the in vivo system, our biochemical analyses were performed in a heterologous system using truncated dBruce versions, and thus, we cannot completely rule out the possibility that at least some of the ubiquitinated dBruce is degraded by the proteasome. However, our genetic data support a model where dBruce may be redistributed by an active translocation mechanism, as hyperactivation of the Cullin-3-based complex, following Soti inactivation, leads to accumulation of dBruce at tail ends of spermatids and not to its elimination. This idea is also indirectly supported from the experiment in the eye system, showing that transgenic expression of the dBruce mini-gene enhanced the small eye phenotype caused by expression of Klhl10, suggesting that the Cullin-3-based complex does not target the dBruce mini-gene for degradation in this system. Consistent with this notion, accumulating evidence indicates that the ubiquitin "code" on target proteins can be read by a large number of ubiquitin-binding proteins, which translate the ubiquitin code to specific cellular outputs, such as protein redistribution (for review, see Hurley et al., 2006; Chen and Sun, 2009). Interestingly, a recent report suggests that Cullin-3-based polyubiquitination of caspase-8 promotes its aggregation, which subsequently leads to processing and full activation of this protease (Jin et al., 2009). Furthermore, another Cullin-3-based ubiquitin ligase complex was shown to regulate the dynamic localization of the Aurora B kinase on mitotic chromosomes (Sumara et al., 2007). Therefore, Cullin-3-based ubiquitin ligase complexes appear to promote also nondegradative ubiquitination and redistribution of proteins.

## Soti Behaves as a Pseudosubstrate Inhibitor of the Cullin-3-Based E3 Ubiquitin ligase Complex

Cullin-RING ubiquitin ligases (CRLs) bind to substrates via adaptor proteins (Willems et al., 2004; Cardozo and Pagano, 2004; Petroski and Deshaies, 2005). However, adaptor proteins can also bind to pseudosubstrate inhibitors in a manner which is reminiscent of an E3-substrate-type interaction (Davis et al., 2002; Miller et al., 2006; Burton and Solomon, 2007; Malureanu et al., 2009). Several lines of evidence strongly suggest that Soti is a pseudosubstrate inhibitor of the Cullin-3-based E3 ubiquitin ligase complex in spermatids. First, the interaction between Klhl10 and Soti is an E3-substrate-type interaction. Second, Soti is not a substrate for this E3 complex. Third, dBruce polypeptides can outcompete with Soti for binding to Klhl10. Finally, Soti is a potent inhibitor of this E3 complex. Therefore, the mechanism of regulation by pseudosubstrates may represent a more common mechanism for modulation of CRL activity than has been previously appreciated.

## Soti Is Degraded by a Noncanonical Degradation Pathway

Two alternative protein degradation pathways were recently described: N-terminal ubiquitination (NTU) and degradation "by default." Whereas the former promotes degradation of proteins by ubiquitination at N-terminal residues, the latter targets proteins for degradation by a ubiquitin-independent, 20S proteasome-dependent mechanism (Ciechanover, 2005; Asher et al., 2006). Although our results cannot conclusively distinguish between these two pathways, two notable mechanistic traits of degradation "by default" can be also attributed to Soti, including the targeting of intrinsically disordered proteins and their protection by binding to other proteins ("nannies") (Tsvetkov et al., 2009). Using the FoldIndex tool (see also in the Experimental Procedures), Soti was predicted to be intrinsically disordered, while it is stabilized by attachment of a structured Myc-tag to its N terminus. Furthermore, Soti is highly unstable in the absence of its binding partner Klhl10, suggesting that Klhl10 functions as a "nanny" for its own inhibitor.

In conclusion, we have uncovered a mechanism that restricts caspase activation during the vital process of spermatid individualization. This process appears to be conserved both anatomically and molecularly from *Drosophila* to mammals (reviewed in detail in Feinstein-Rotkopf and Arama, 2009). Moreover, several recent studies suggest that a similar Klhl10-Cul3 complex is essential for late spermatogenesis in mammals (Yan et al., 2004; Wang et al., 2006; Yatsenko et al., 2006). Therefore, although the mammalian sperm is about 30 times shorter than

in *Drosophila*, similar mechanisms (albeit scaled-down) for regulation of caspase activation may also exist during mammalian spermatogenesis. Further studies of the link between the ubiquitin pathway and apoptotic proteins during sperm differentiation in *Drosophila* may, therefore, provide new insights into the etiology of some forms of human infertility.

## EXPERIMENTAL PROCEDURES

### Fly Strains and Expression Vectors

*yw* flies were used as wild-type controls. The *Df*(3R)Exel6267 line was obtained from the Bloomington Stock Center. The *cul3*$^{mds1}$, *cul3*$^{mds5}$, *cul3*$^{gft2}$, *cul3*$^{gft06430}$, *klhl10*$^{3}$, and *klhl10*$^{4}$ mutants are described in (Arama et al., 2007). The *jar*$^{1}$ mutant is described in (Hicks et al., 1999).

The *soti*$^{sik}$ mutant line was generated by an imprecise excision of the *P*{XP}d01837 insertion, using the transposase-producing *Δ2-3* 'jumpstart' strain, essentially as described in Torok et al. (1993). One out of 68 independent imprecisely excision lines contained a 1393 bp deletion at the *soti* locus.

Generation of all the constructs and transgenes that are mentioned in this study are described in detail in the Supplemental Information.

### Yeast-Two-Hybrid Screen

The two-hybrid screen was performed using *S. cerevisiae* strain AH109 and an adult *Drosophila* cDNA library (Matchmaker, Clontech). Selection was done on synthetic complete medium lacking tryptophan, leucine, histidine, and adenine for 4 days at 30°C. The Klhl10 "bait" construct contains a fragment of *klhl10* ORF that lacks the BTB domain (amino acids 188–767). Similarly, baits with mutated forms of Klhl10, designated S480F, G496R, and E601K were generated and which correspond to the *klhl10* mutant alleles *klhl10*$^{6}$, *klhl10*$^{5}$, and *klhl10*$^{2}$, respectively (Arama et al., 2007). More details are found in the Supplemental Information.

### Immunofluorescence Staining and Antibodies

Whole-mount immunofluorescence staining of young (0–2 day old) adult testes was carried out as described in (Arama et al., 2007). The antibodies used are rabbit polyclonal anti-cleaved Caspase-3 (Asp175, Cell Signaling Technology; 1:75), mouse monoclonal AXO 49 (a gift from Marie-Helene Bre, University of Paris-Sud, France; 1:5000), mouse monoclonal anti-c-Myc (clone 9E10; Santa Cruz Biotechnology; 1:50), guinea pig polyclonal affinity-purified anti-Soti (1:100), and rabbit polyclonal dBruce anti-serum (B710; 1:500). The last two antibodies were generated in this study (see details in Supplemental Information).

For immunohistochemistry of testis sections, see details in Supplemental Information.

### Western Blotting and IP Experiments in S2 Cells

Testis protein extracts were prepared from 60–80 adult testes as described in (Arama et al., 2007).

S2 cells were grown in standard Schneider's *Drosophila* Medium (Biological Industries, Israel) supplemented with 10% FBS (GIBCO). Cells (4.5–5×10$^{6}$ per 50 ml flask) were transfected using the Escort IV reagent (Sigma-Aldrich) according to the manufacturer's instructions. Cells were lysed 48 hr posttransfection in NP-40 buffer (10 mM HEPES [pH 7.4], 1 mM $MgCl_2$, 100 mM NaCl, 1% Igepal CA-360, and a protease inhibitor mix). Extracts were incubated ON at 4°C with Dynabeads either conjugated to Protein G (Dynal, Invitrogen), bound to rabbit polyclonal anti-GFP antibody (ab290, Abcam), or conjugated to Sheep anti-Rabbit IgG (Dynal, Invitrogen). The beads were washed, and bound proteins were eluted by boiling in SDS-PAGE loading buffer and subjected to western blotting. The following antibodies were used for immunoblotting: guinea pig anti-Soti antibody (this study; 1:1000), mouse anti-c-Myc (clone 9E10; Santa Cruz Biotechnology; 1:1000), mouse anti-*Drosophila* β-tubulin (clone E7 s, Hybridoma Bank; 1:000), mouse anti-GFP (clones 7.1 and 13.1; Roche Applied Science; 1:1000), mouse anti-HA (HA.11 clone 16B12, Covance; 1:1000), rat anti-dBruce [Arama et al., 2007]; 1:1000), and mouse anti-CUL-3 (BD Transduction Laboratories; 1:1000).

### Ubiquitination Assay

S2 cells at 40 hr after transfection were treated with 50 μM MG132 (Sigma-Aldrich) for additional 4–6 hr. Cells were then harvested and lysed by boiling for 10 min in SDS buffer (2% SDS, 20 mM EDTA, 50 mM Tris [pH 8.0], 20 mM DTT, 500 mM NEM, and a mix of protease inhibitors). The lysates were sonicated, diluted 1/10 in TNN buffer (50 mM Tris [pH 7.5], 120 mM NaCl, 5 mM EDTA, 0.5% Igepal, 1 mM DTT, and a protease inhibitor mix), and centrifuged. The supernatants were immunoprecipitated using mouse anti-HA-conjugated agarose (clone HA-7, Sigma-Aldrich) ON at 4°C. After three washes with TNN buffer, bound proteins were eluted by boiling in SDS-PAGE loading buffer and subjected to western blotting by using mouse anti-FLAG Ab (clone M2, Sigma-Aldrich; 1:1000) or rabbit anti-HA Ab (Sigma-Aldrich; 1:1000).

### Eye Images

Heads of young females (0–2 day old) were disconnected from the body using a scalpel and cut again on a slide to separate the two eyes. Images were obtained using a stereo microscope (MZ16F; Leica) connected to a DS-Fi1 camera (Nikon).

### Prediction of Intrinsically Unfolded Proteins

FoldIndex: a simple tool to predict whether a given protein sequence is intrinsically unfolded. http://bioportal.weizmann.ac.il/fldbin/findex.

## SUPPLEMENTAL INFORMATION

Supplemental Information includes Supplemental Experimental Procedures and five figures and can be found online at doi:10.1016/j.devcel.2010.06.009.

## ACKNOWLEDGMENTS

We are grateful to Johannes Bischof, Marie-Helene Bre, Robert Duronio, Gregory C. Rogers, Herman Steller, and the Bloomington stock center for providing additional stocks and reagents. We sincerely acknowledge Nitzan Adam for technical help, Shari Carmon for help with establishment of the S2 cell system, and Orith Leitner and Ziv Landau in the antibody unit at the WIS. We thank the Arama lab members for encouragement and advice. The help and advice from Amir Orian, Yosef Shaul, and Avraham Yaron are also greatly appreciated. We are deeply indebted to Orly Reiner and Ben-Zion Shilo for critically reading the manuscript, fruitful discussions, and useful advice. We warmly thank Samara Brown for editing the manuscript. This research was supported in part by the Legacy Heritage Fund Program of the Israel Science Foundation (Grant No. 1498/06), the Israel Science Foundation – Keren Dorot (Grant No. 308/09), Minerva foundation with funding from the Federal German Ministry for Education and Research, Israel Cancer Research Fund, German-Israeli Foundation for Scientific Research and Development, and the Moross Institute for Cancer Research. E.A. is an Alon Fellow with the Council for Higher Education of the Israeli Academy of Sciences and is also supported by grants from Lord Mitchell, The Henry S. & Anne S. Reich Research Fund for Mental Health, The Samuel M. Soref & Helene K. Soref Foundation, and The Chais Family Fellows Program for New Scientists. E.A. is the Incumbent of the Corinne S. Koshland Career Development Chair. Y.F.-R. receives funding from the Israeli Ministry of Absorption in Science. We apologize to those whose work we did not cite because of either oversight on our part or space constraints.

Received: November 3, 2009
Revised: March 25, 2010
Accepted: May 4, 2010
Published: July 19, 2010

## REFERENCES

Arama, E., Agapite, J., and Steller, H. (2003). Caspase activity and a specific cytochrome C are required for sperm differentiation in Drosophila. Dev. Cell *4*, 687–697.

Arama, E., Bader, M., Srivastava, M., Bergmann, A., and Steller, H. (2006). The two Drosophila cytochrome C proteins can function in both respiration and caspase activation. EMBO J. *25*, 232–243.

Arama, E., Bader, M., Rieckhof, G.E., and Steller, H. (2007). A ubiquitin ligase complex regulates caspase activation during sperm differentiation in Drosophila. PLoS Biol. *5*, e251. 10.1371/journal.pbio.0050251.

Asher, G., Reuven, N., and Shaul, Y. (2006). 20S proteasomes and protein degradation "by default". Bioessays *28*, 844–849.

Baehrecke, E.H. (2002). How death shapes life during development. Nat. Rev. Mol. Cell Biol. *3*, 779–787.

Barreau, C., Benson, E., Gudmannsdottir, E., Newton, F., and White-Cooper, H. (2008). Post-meiotic transcription in Drosophila testes. Development *135*, 1897–1902.

Bartke, T., Pohl, C., Pyrowolakis, G., and Jentsch, S. (2004). Dual role of BRUCE as an antiapoptotic IAP and a chimeric E2/E3 ubiquitin ligase. Mol. Cell *14*, 801–811.

Bergmann, A., Yang, A.Y., and Srivastava, M. (2003). Regulators of IAP function: coming to grips with the grim reaper. Curr. Opin. Cell Biol. *15*, 717–724.

Bloom, J., Amador, V., Bartolini, F., DeMartino, G., and Pagano, M. (2003). Proteasome-mediated degradation of p21 via N-terminal ubiquitinylation. Cell *115*, 71–82.

Bosu, D.R., and Kipreos, E.T. (2008). Cullin-RING ubiquitin ligases: global regulation and activation cycles. Cell Div. *3*, 7.

Breitschopf, K., Bengal, E., Ziv, T., Admon, A., and Ciechanover, A. (1998). A novel site for ubiquitination: the N-terminal residue, and not internal lysines of MyoD, is essential for conjugation and degradation of the protein. EMBO J. *17*, 5964–5973.

Burton, J.L., and Solomon, M.J. (2007). Mad3p, a pseudosubstrate inhibitor of APCCdc20 in the spindle assembly checkpoint. Genes Dev. *21*, 655–667.

Cardozo, T., and Pagano, M. (2004). The SCF ubiquitin ligase: insights into a molecular machine. Nat. Rev. Mol. Cell Biol. *5*, 739–751.

Chen, Z.J., and Sun, L.J. (2009). Nonproteolytic functions of ubiquitin in cell signaling. Mol. Cell *33*, 275–286.

Ciechanover, A. (2005). N-terminal ubiquitination. Methods Mol. Biol. *301*, 255–270.

Davis, M., Hatzubai, A., Andersen, J.S., Ben-Shushan, E., Fisher, G.Z., Yaron, A., Bauskin, A., Mercurio, F., Mann, M., and Ben-Neriah, Y. (2002). Pseudosubstrate regulation of the SCF(beta-TrCP) ubiquitin ligase by hnRNP-U. Genes Dev. *16*, 439–451.

Donaldson, T.D., Noureddine, M.A., Reynolds, P.J., Bradford, W., and Duronio, R.J. (2004). Targeted disruption of Drosophila Roc1b reveals functional differences in the Roc subunit of Cullin-dependent E3 ubiquitin ligases. Mol. Biol. Cell *15*, 4892–4903.

Fabrizio, J.J., Hime, G., Lemmon, S.K., and Bazinet, C. (1998). Genetic dissection of sperm individualization in Drosophila melanogaster. Development *125*, 1833–1843.

Feinstein-Rotkopf, Y., and Arama, E. (2009). Can't live without them, can live with them: roles of caspases during vital cellular processes. Apoptosis *14*, 980–995.

Gilbert, S.F. (2001). Developmental Biology (Sunderland, MA: Sinauer Associates).

Glickman, M.H., and Ciechanover, A. (2002). The ubiquitin-proteasome proteolytic pathway: destruction for the sake of construction. Physiol. Rev. *82*, 373–428.

Goyal, L. (2001). Cell death inhibition: keeping caspases in check. Cell *104*, 805–808.

Hao, Y., Sekine, K., Kawabata, A., Nakamura, H., Ishioka, T., Ohata, H., Katayama, R., Hashimoto, C., Zhang, X., Noda, T., et al. (2004). Apollon ubiquitinates SMAC and caspase-9, and has an essential cytoprotection function. Nat. Cell Biol. *6*, 849–860.

Hicks, J.L., Deng, W.M., Rogat, A.D., Miller, K.G., and Bownes, M. (1999). Class VI unconventional myosin is required for spermatogenesis in Drosophila. Mol. Biol. Cell *10*, 4341–4353.

Huh, J.R., Vernooy, S.Y., Yu, H., Yan, N., Shi, Y., Guo, M., and Hay, B.A. (2004). Multiple apoptotic caspase cascades are required in nonapoptotic roles for Drosophila spermatid individualization. PLoS Biol. *2*, E15.

Hurley, J.H., Lee, S., and Prag, G. (2006). Ubiquitin-binding domains. Biochem. J. *399*, 361–372.

Jacobson, M.D., Weil, M., and Raff, M.C. (1997). Programmed cell death in animal development. Cell *88*, 347–354.

Jin, Z., Li, Y., Pitti, R., Lawrence, D., Pham, V.C., Lill, J.R., and Ashkenazi, A. (2009). Cullin3-based polyubiquitination and p62-dependent aggregation of caspase-8 mediate extrinsic apoptosis signaling. Cell *137*, 721–735.

Kuranaga, E., and Miura, M. (2007). Nonapoptotic functions of caspases: caspases as regulatory molecules for immunity and cell-fate determination. Trends Cell Biol. *17*, 135–144.

Malureanu, L.A., Jeganathan, K.B., Hamada, M., Wasilewski, L., Davenport, J., and van Deursen, J.M. (2009). BubR1 N terminus acts as a soluble inhibitor of cyclin B degradation by APC/C(Cdc20) in interphase. Dev. Cell *16*, 118–131.

Merlet, J., Burger, J., Gomes, J.E., and Pintard, L. (2009). Regulation of cullin-RING E3 ubiquitin-ligases by neddylation and dimerization. Cell Mol. Life Sci. *66*, 1924–1938.

Miller, J.J., Summers, M.K., Hansen, D.V., Nachury, M.V., Lehman, N.L., Loktev, A., and Jackson, P.K. (2006). Emi1 stably binds and inhibits the anaphase-promoting complex/cyclosome as a pseudosubstrate inhibitor. Genes Dev. *20*, 2410–2420.

Morgan, M.J., and Thorburn, A. (2001). Measurement of caspase activity in individual cells reveals differences in the kinetics of caspase activation between cells. Cell Death Differ. *8*, 38–43.

Muro, I., Berry, D.L., Huh, J.R., Chen, C.H., Huang, H., Yoo, S.J., Guo, M., Baehrecke, E.H., and Hay, B.A. (2006). The Drosophila caspase Ice is important for many apoptotic cell deaths and for spermatid individualization, a nonapoptotic process. Development *133*, 3305–3315.

Noguchi, T., and Miller, K.G. (2003). A role for actin dynamics in individualization during spermatogenesis in Drosophila melanogaster. Development *130*, 1805–1816.

Petroski, M.D., and Deshaies, R.J. (2005). Function and regulation of cullin-RING ubiquitin ligases. Nat. Rev. Mol. Cell Biol. *6*, 9–20.

Pintard, L., Willems, A., and Peter, M. (2004). Cullin-based ubiquitin ligases: Cul3-BTB complexes join the family. EMBO J. *23*, 1681–1687.

Pitnick, S., Spicer, G.S., and Markow, T.A. (1995). How long is a giant sperm? Nature *375*, 109.

Raff, M. (1998). Cell suicide for beginners. Nature *396*, 119–122.

Rogowski, K., Juge, F., van, D.J., Wloga, D., Strub, J.M., Levilliers, N., Thomas, D., Bre, M.H., Van, D.A., Gaertig, J., and Janke, C. (2009). Evolutionary divergence of enzymatic mechanisms for posttranslational polyglycylation. Cell *137*, 1076–1087.

Salvesen, G.S., and Riedl, S.J. (2008). Caspase mechanisms. Adv. Exp. Med. Biol. *615*, 13–23.

Sumara, I., Quadroni, M., Frei, C., Olma, M.H., Sumara, G., Ricci, R., and Peter, M. (2007). A Cul3-based E3 ligase removes Aurora B from mitotic chromosomes, regulating mitotic progression and completion of cytokinesis in human cells. Dev. Cell *12*, 887–900.

Tittel, J.N., and Steller, H. (2000). A comparison of programmed cell death between species. Genome Biol. *1*, reviews0003.1–reviews0003.6.

Tokuyasu, K.T., Peacock, W.J., and Hardy, R.W. (1972). Dynamics of spermiogenesis in Drosophila melanogaster. I. Individualization process. Z. Zellforsch. Mikrosk. Anat. *124*, 479–506.

Torok, T., Tick, G., Alvarado, M., and Kiss, I. (1993). P-lacW insertional mutagenesis on the second chromosome of Drosophila melanogaster: isolation of lethals with different overgrowth phenotypes. Genetics *135*, 71–80.

Tsvetkov, P., Reuven, N., and Shaul, Y. (2009). The nanny model for IDPs. Nat. Chem. Biol. *5*, 778–781.

Wang, S., Zheng, H., Esaki, Y., Kelly, F., and Yan, W. (2006). Cullin3 is a KLHL10-interacting protein preferentially expressed during late spermiogenesis. Biol. Reprod. *74*, 102–108.

Willems, A.R., Schwab, M., and Tyers, M. (2004). A hitchhiker's guide to the cullin ubiquitin ligases: SCF and its kin. Biochim. Biophys. Acta *1695*, 133–170.

Wu, J.T., Chan, Y.R., and Chien, C.T. (2006). Protection of cullin-RING E3 ligases by CSN-UBP12. Trends Cell Biol. *16*, 362–369.

Yan, W., Ma, L., Burns, K.H., and Matzuk, M.M. (2004). Haploinsufficiency of kelch-like protein homolog 10 causes infertility in male mice. Proc. Natl. Acad. Sci. USA *101*, 7793–7798.

Yatsenko, A.N., Roy, A., Chen, R., Ma, L., Murthy, L.J., Yan, W., Lamb, D.J., and Matzuk, M.M. (2006). Non-invasive genetic diagnosis of male infertility using spermatozoal RNA: KLHL10 mutations in oligozoospermic patients impair homodimerization. Hum. Mol. Genet. *15*, 3411–3419.

Yi, C.H., and Yuan, J. (2009). The Jekyll and Hyde functions of caspases. Dev. Cell *16*, 21–34.

Yin, V.P., and Thummel, C.S. (2005). Mechanisms of steroid-triggered programmed cell death in Drosophila. Semin. Cell Dev. Biol. *16*, 237–243.

**Developmental Cell *19***

# Supplemental Information

# Gradients of an Ubiquitin E3 Ligase Inhibitor and a Caspase Inhibitor Determine Differentiation or Death in Spermatids

**Yosef Kaplan, Liron Gibbs-Bar, Yossi Kalifa, Yael Feinstein-Rotkopf, and Eli Arama**

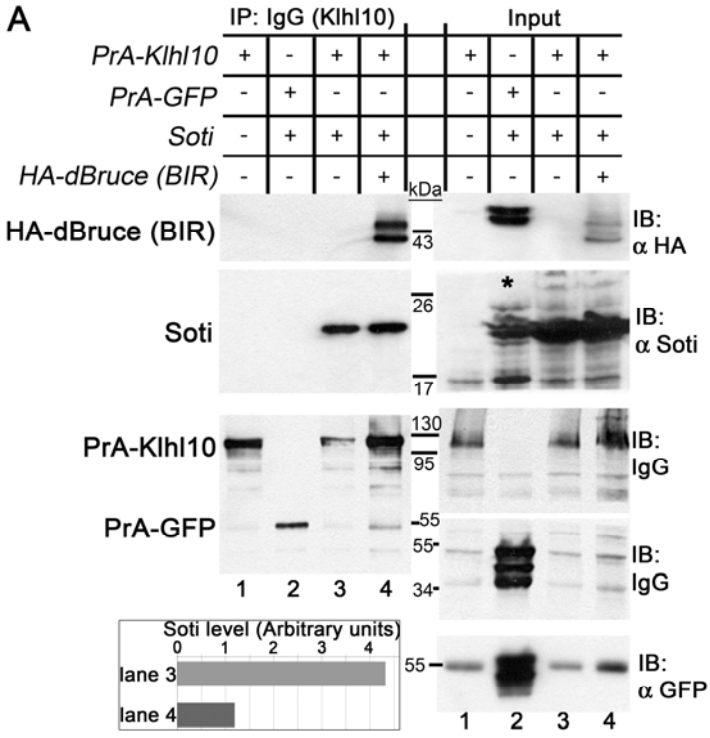


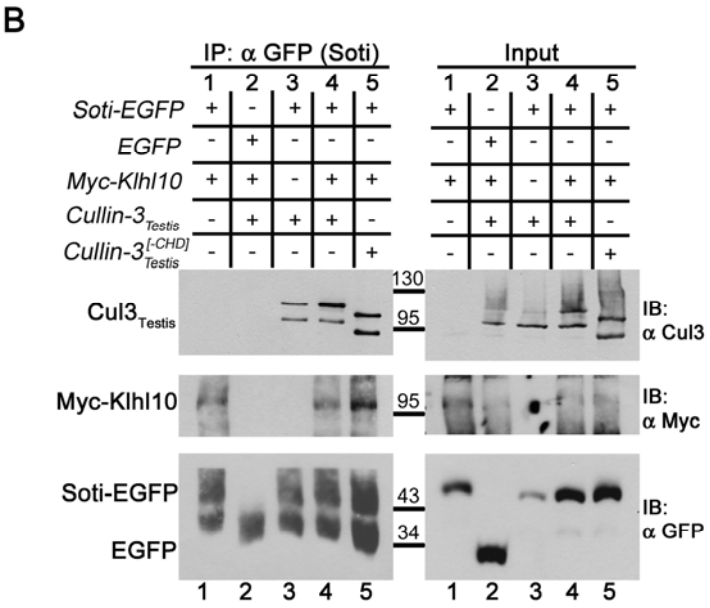

**Figure S1. Klhl10 Forms Complexes with Soti, $Cul3_{Testis}$, and dBruce, related to Figure 1**

(A) Co-IP experiment in S2 cells which were co-transfected with constructs encoding Protein A (PrA)-tagged Klhl10 (or PrA-tagged GFP as control), non-tagged Soti, and HA-tagged dBruce (BIR) polypeptide (for details about the latter see the scheme and legends in Figure 7A). PrA immunoprecipitates ('IP') and the corresponding pre-incubated lysates ('Input') were analyzed by immunoblotting with the indicated antibodies (denoted as 'IB' at the right). A GFP construct was co-transfected and used to asses transfection efficiency and loading levels (bottom panel in the 'Input'). Both Soti and dBruce (BIR) are present in immunoprecipitates of PrA-Klhl10. The graph in the bottom indicates the relative levels of co-precipitated Soti in lanes 3 and 4 after normalization according the corresponding levels of the immunoprecipitated PrA-Klhl10. Note that coexpression of dBruce 'BIR' caused to 3.6-fold decrease in the level of Soti that binds to Klhl10.

(B) Soti can interact with neddylated and non-neddylated Klhl10-Cul3 complex. Shown is an immunoblot of anti-GFP coimmunoprecipitation assay. S2 cells were co-transfected with EGFP-tagged Soti, Myc-tagged Klhl10 and either non-tagged intact $Cul3_{Testis}$ or a mutated $Cul3_{Testis}$, which lacks the CHD domain and hence is incapable of interacting with the RING protein and forming an active complex ($Cul3_{Testis}^{[-CHD]}$; the CHD region includes the conserved neddylatable lysine residue). EGFP was used as negative control for the co-IP (lane 2). Anti-GFP Ab was used to immunoprecipitate the Soti complex, while the presence of the Cullin-3 in the immunoprecipitate (IP) was detected using the anti-Cul3 Ab. Pre-incubated lysates are shown to the right (Input). Soti can co-precipitate with both the neddylated and non-neddylated Cullin-3 even in the absence of exogenous Klhl10, implying that some level of endogenous Klhl10 may be present in these cells (IP, lane 3, upper and lower bands, respectively). Co-transfection of Klhl10 increases the level of Cullin-3 in the Soti immunoprecipitate, in particular the level of the higher, neddylated, form (IP, lane 4). Soti could also interact with the inactive Cullin-3, suggesting that its interaction with the Cul3 complex is independent of the activation state of Cullin-3 (IP, lane 5). Note that this Cul3 mutant also exhibits two forms, although it lacks the conserved neddylatable lysine, implying that it may be neddylated on an alternative lysine residue.

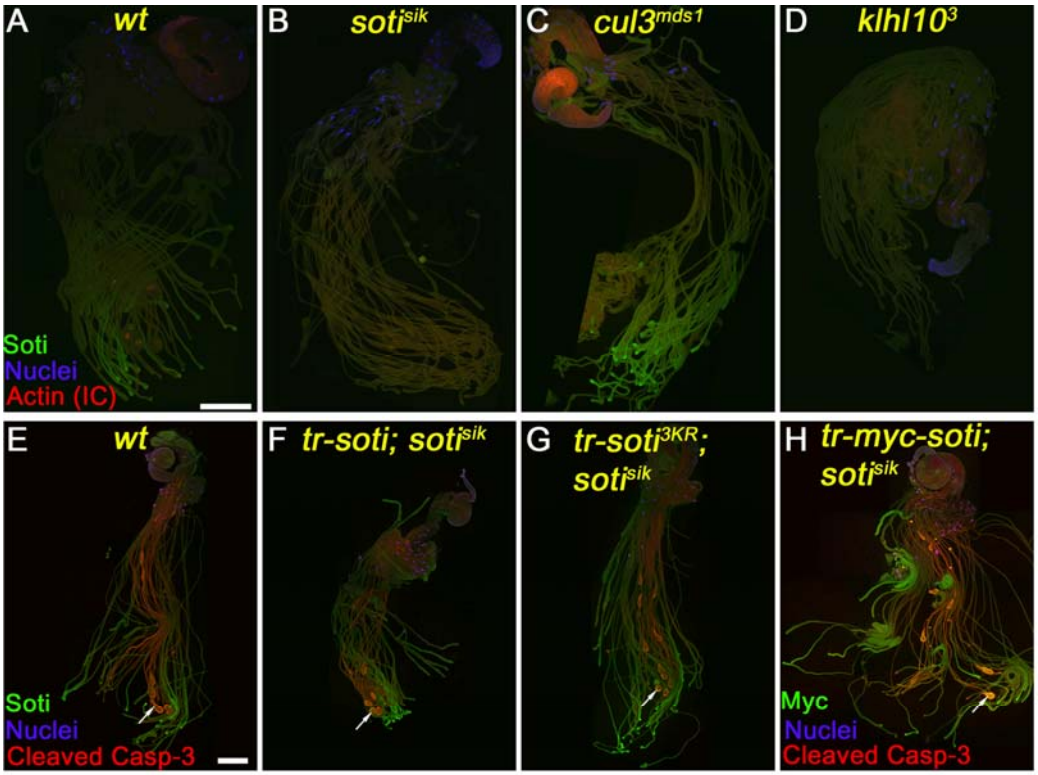


I

| | 1 | 2 | 3 | 4 | 5 | 6 |
|---|---|---|---|---|---|---|
| *Soti* | - | - | + | - | + | - |
| *Cullin-3$^{[-CHD]}_{Testis}$* | - | - | - | - | - | + |
| *Cullin-3$_{Testis}$* | - | - | - | + | + | - |
| *Roc1a* | - | - | - | + | + | + |
| *HA-Klhl10* | - | + | + | + | + | + |
| *3xFlag-Ub* | + | + | + | + | + | + |
| *MG132* | + | + | + | + | + | + |

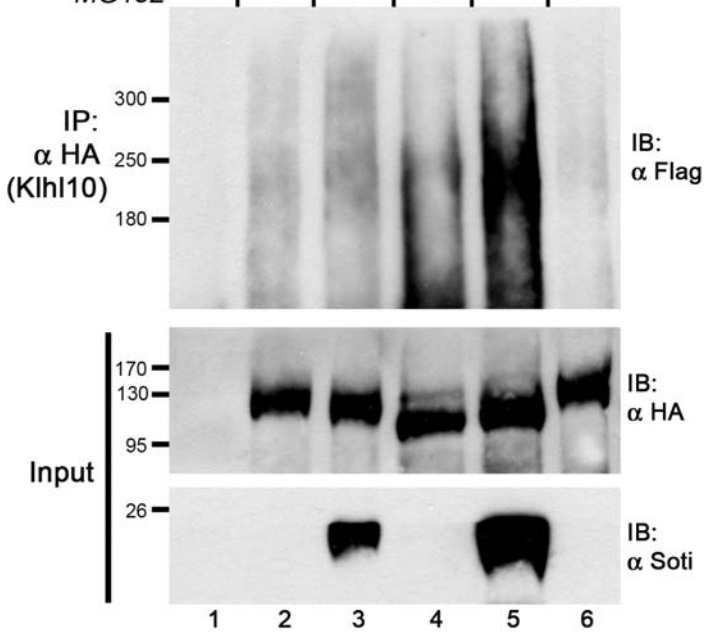

**Figure S2. Soti is Absent in *klhl10* Mutant Spermatids and is Stabilized in *cullin-3* Mutants, related to Figure 3**

(A-D) Spermatids were stained to visualize Soti (green), ICs (red), and nuclei (blue). (A) Soti is detected in wild-type spermatids and (B) absent in $soti^{sik}$ mutants. (C) Consistent with the Western blotting analysis, Soti protein level is elevated in $cul3^{mds1}$ mutant spermatids, albeit it is still distributed in a gradient. (D) As was demonstrated in the Western blotting experiment, no Soti protein is detected in $klhl10^{3}$ mutant spermatids. Scale bar, 200 μm.

(E-H) All of the *soti*-related transgenic constructs indicated can rescue spermatid individualization and fertility in $soti^{sik}$ mutants. Spermatids were stained with anti-Soti (E-G) or anti-Myc (H) antibodies to visualize the different Soti transgenes (green), anti-cleaved caspase-3 to visualize active effector caspase (red), and DAPI (nuclei; blue). Note that all transgenes are distributed in similar gradients (green) and the appearance of "normal" oval cystic bulges and waste bags (red; arrows). Scale bar, 200 μm.

(I) Klhl10 undergoes autoubiquitination which is not affected by Soti. S2 cells were co-transfected with HA-tagged Klhl10 and one or more of the following: Roc1a, $Cul3_{Testis}$ or the catalytically inactive $Cul3_{Testis}^{[-CHD]}$, and Soti. In addition, all cells were co-transfected with Flag-Ub, and at 40 hours post-transfection incubated with the proteasome inhibitor MG132 for 6 hours. Cells were lysed under denaturing conditions and Klhl10 was isolated with anti-HA beads. The presence of Klhl10 or its ubiquitinated forms were identified by immunoblotting with the anti-HA or anti-Flag Abs, respectively. Although Klhl10 is ubiquitinated in the absence of exogenous $Cul3_{Testis}$ and Roc1a (lane 2), its ubiquitination remarkably increases following co-transfection of these two constructs (lane 4). The autoubiquitination in lane 2 is attributed to endogenous Cullin-3 and Roc proteins, as it is strongly attenuated in the presence of the dominant-negative form of $Cul3_{Testis}$ (lane 6). Co-transfection of Soti does not interfere with autoubiquitination of Klhl10 (lanes 3 and 5).

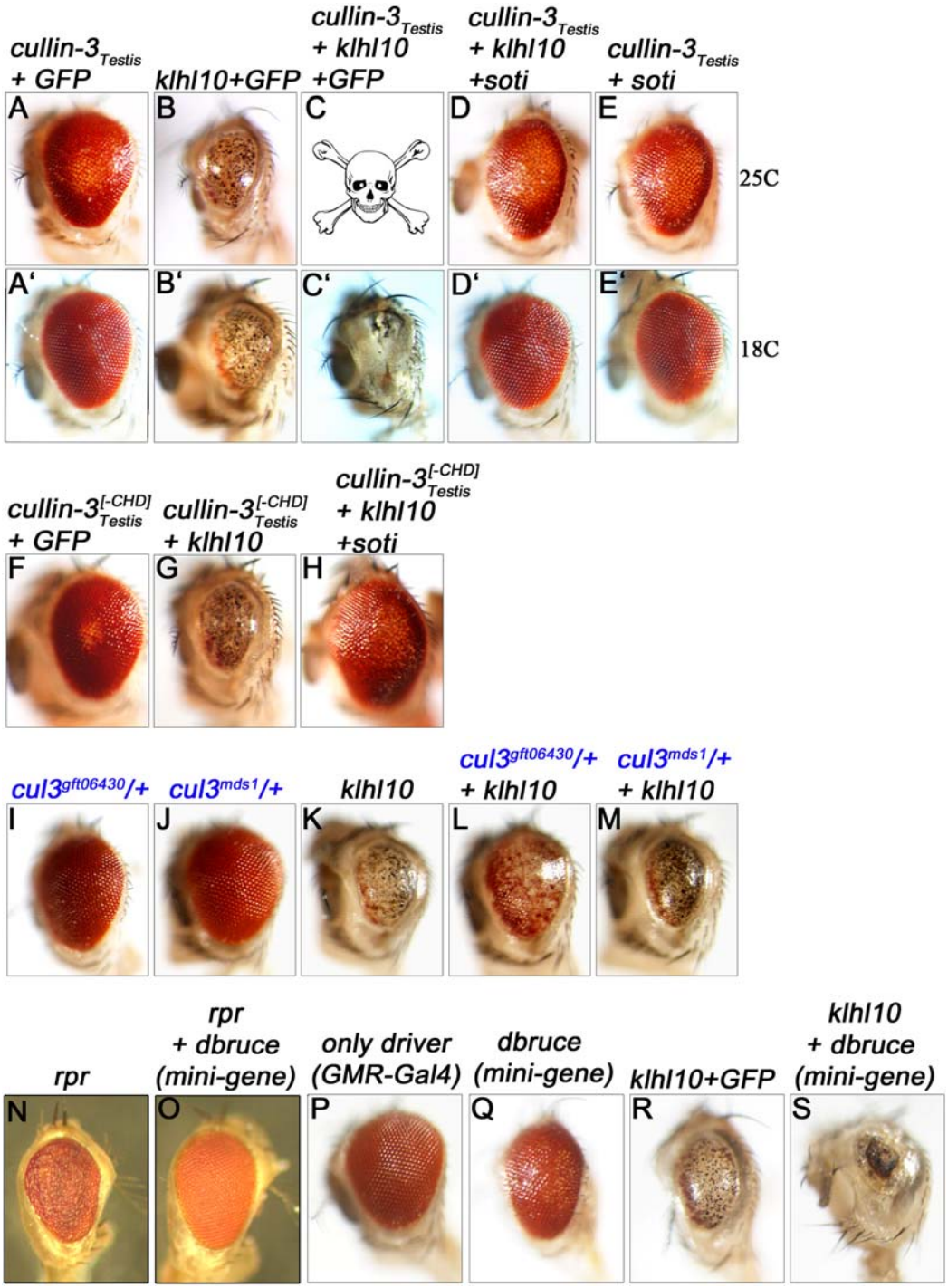


**Figure S3. Soti can Inhibit the Cullin-3–Based Ubiquitin Ligase Complex in an Ectopic System, related to Figure 4**

(A-M) Transgenesis experiments using the *Drosophila* adult compound eye. The names of the ectopically expressed genes in each experiment are in black captions above each panel, while blue captions describe the genotype backgrounds if different than wild-type. In all of the experiments, two copies of the GMR-Gal4 driver were used to drive expression of single copies of the UAS-dependent transgenes in the eye imaginal disc. A UAS-*GFP* line was used to control for possible sequestering of the

GAL4 due to the presence of several UAS-transgenic lines. Flies were reared at 25°C unless otherwise indicated. Representative eyes from newly eclosed female flies are shown.

(A-E and A'-E') Expression of *soti* completely suppresses the strong eye phenotypes caused by the combined expression of the testis-specific isoform of *cullin-3* (*cul3*$_{Testis}$) and *klhl10*. The eyes shown in (A-E) and (A'-E') are from the same respective fly lines. One set of flies was reared at 25°C (A-E), while the other at 18°C, to reduce the strong synergistic effect (A'-E').

(A, A') Transgenic expression of *cul3*$_{Testis}$ in the eye causes very minor morphological alterations (slight glossiness and roughness of the eyes) at 25°C (A) and no apparent effects at 18°C (A').

(B, B') The strong *klhl10* effect (B) is only slightly attenuated at 18°C (B').

(C, C') Combined expression of *cul3*$_{Testis}$ and *klhl10* results in larval lethality at 25°C (C) and almost complete eye ablation at 18°C (C').

(D, D') *soti* expression completely suppresses the lethality (D) and ablated eye phenotype (D') caused by the combined expression of *cul3*$_{Testis}$ and *klhl10*.

(E, E') *soti* does not suppress the slight eye glossiness and roughness in *cul3*$_{Testis}$ transgenic flies (E), suggesting that this effect is independent of Klhl10.

(F-H) The synergistic effect between Cullin-3 and Klhl10 requires assembly of an active Cullin-3–based complex. (F) Transgenic expression of a catalytically inactive *cul3*$_{Testis}$ (*cul3*$_{Testis}^{[-CHD]}$), which lacks the C-terminal Cullin-homology-domain (CHD), causes minor morphological defects reminiscent of expression of *cul3*$_{Testis}$, suggesting that the slight eye glossiness and roughness in *cul3*$_{Testis}$ transgenic flies are unrelated to its catalytic activity. (G) Transgenic expression of *cul3*$_{Testis}^{[-CHD]}$ does not enhance the eye phenotype of the *klhl10* transgene. (H) *soti* can completely suppress the *klhl10* effect in this background as well.

(I-M) The eye effect of the *klhl10* transgene depends on endogenous expression of the somatic Cullin-3 isoform (Cul3$_{Soma}$) in the eye. (I) Flies heterozygous for the lethal *cullin-3*$_{Soma}$ allele *cul3*$^{gft06430}$ (J) or the male-sterile allele *cul3*$^{mds1}$ display normal eye morphology. For more details about the specific lesions in these alleles see (Arama et al., 2007). (K) Transgenic *klhl10* expression in a wild-type background. (L) Transgenic *klhl10* expression in flies heterozygous for the *cul3*$^{gft06430}$ allele. Note the significant suppression of the *klhl10* eye phenotype. (M) Transgenic *klhl10* expression in flies heterozygous for the *cul3*$^{mds1}$ allele. Note that this allele does not modify the *klhl10* eye phenotype. Therefore, transgenic Klhl10 interacts with eye-resident Cul3$_{Soma}$ and not Cul3$_{Testis}$, in promoting the eye ablation phenotype.

(N-S) Distinct interactions of a dBruce 'mini-gene' with Reaper (Rpr) and Klhl10. The dBruce 'mini-gene' consists of the first N-terminal 1,622 amino acids, including the BIR domain, and the last C-terminal 446 amino acids that contain the UBC domain (see also Figure 6A). (N) Transgenic expression of two copies of a weak *GMR-rpr* transgene causes roughness and partial ablation of the eye (genotype: *GMR-rpr*; *GMR-Gal4*/+). (O) Co-expression of a single copy of the *dbruce 'mini-gene'* remarkably suppressed this Rpr-induced phenotype (genotype: *GMR-rpr*; *GMR-Gal4*/+; *UAS- dbruce 'mini-gene'*/+). (P) A driver line (*2xGMR-Gal4*) exhibits no eye defects, (Q) and addition of two copies of the *dbruce 'mini-gene* resulted in a slightly glossy eye. (R) As shown in (B), addition of two copies of *klhl10* and a single *GFP* to the driver line causes to severe eye phenotype. (S) The eye phenotype in (R) is dramatically enhanced by addition of two copies of the *dbruce 'mini-gene*.

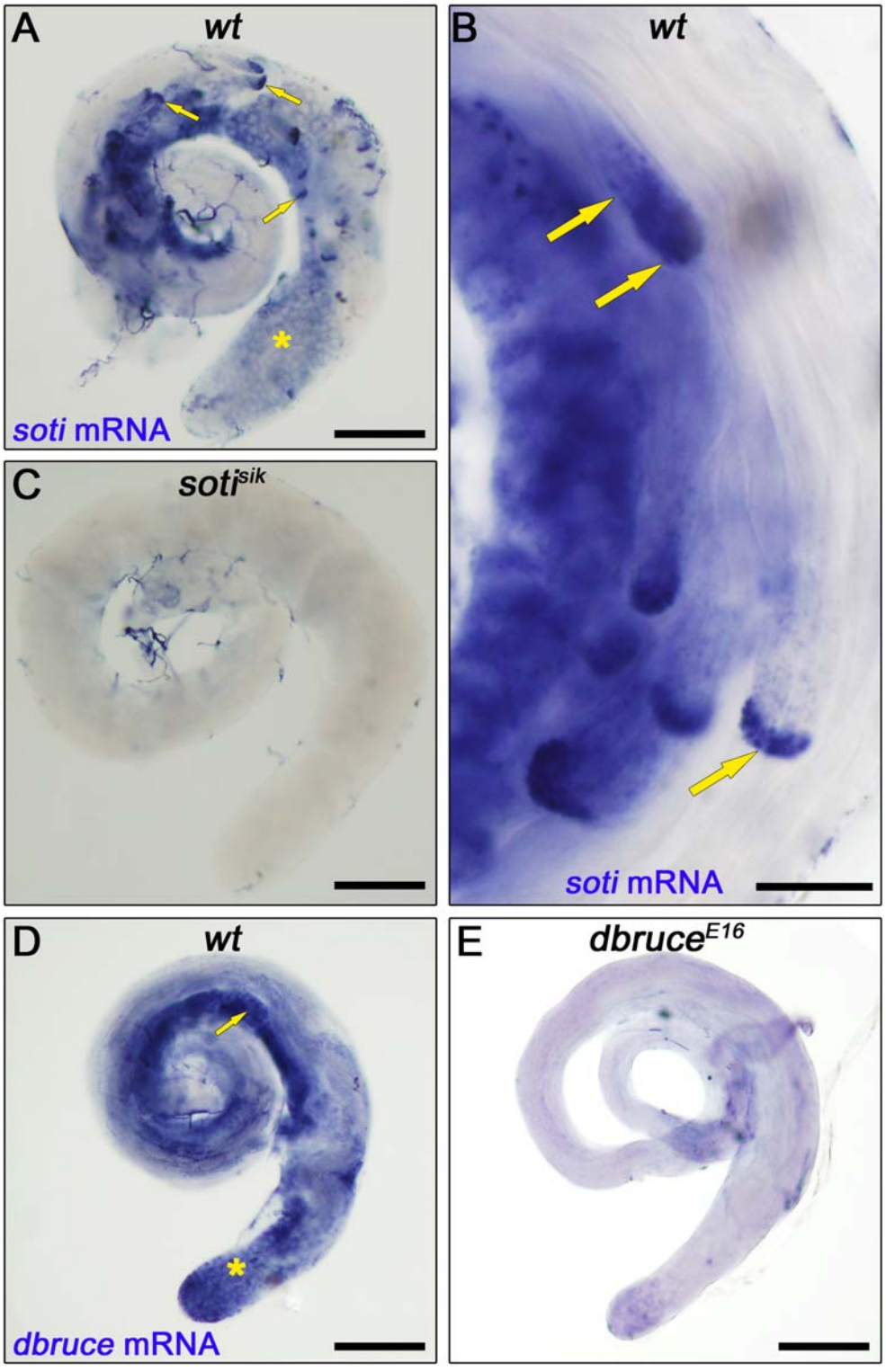


**Figure S4. *soti*, Not *dbruce* Transcripts are Located at Distal (Tail) Ends of Elongating Spermatids, trailing away proximally, related to Figure 5**

(A-E) RNA *in situ* hybridization was performed on whole mount testes from the indicated fly lines using specific *soti* (A-C) and *dbruce* (D, E) probes.

(A, B) In wild-type, *soti* transcripts are detected at very low levels in pre-meiotic primary spermatocytes (the region of these cells is marked by an asterisk). In post-meiotic elongating spermatids the level of *soti* mRNA increases and is confined to the distal (tail) ends, trailing away proximally (arrows).
(C) Consistent with the idea that $soti^{sik}$ is a null *soti* allele, *soti* transcripts are completely absent in testes from these mutants.
(D) In wild-type testes, *dbruce* mRNA is expressed at a similar level in pre-meiotic primary spermatocytes (an asterisk) and elongating spermatids (an arrow). Note that *dbruce* transcripts are uniformly distributed and are not restricted to tail ends.
(E) No *dbruce* signal is detected in testes from a mutant ($dbruce^{E16}$) with a C-terminal deletion in *dbruce* that overlaps with the region of the probe (for more details about the lesion in this mutation see in (Vernooy et al., 2002)). A truncated mRNA of *dbruce* is still expressed in these mutants as was revealed by an RT-PCR experiment (data not shown).
Scale bars in (A, C, D, E), 200 μm. Scale bar in (B), 50 μm.

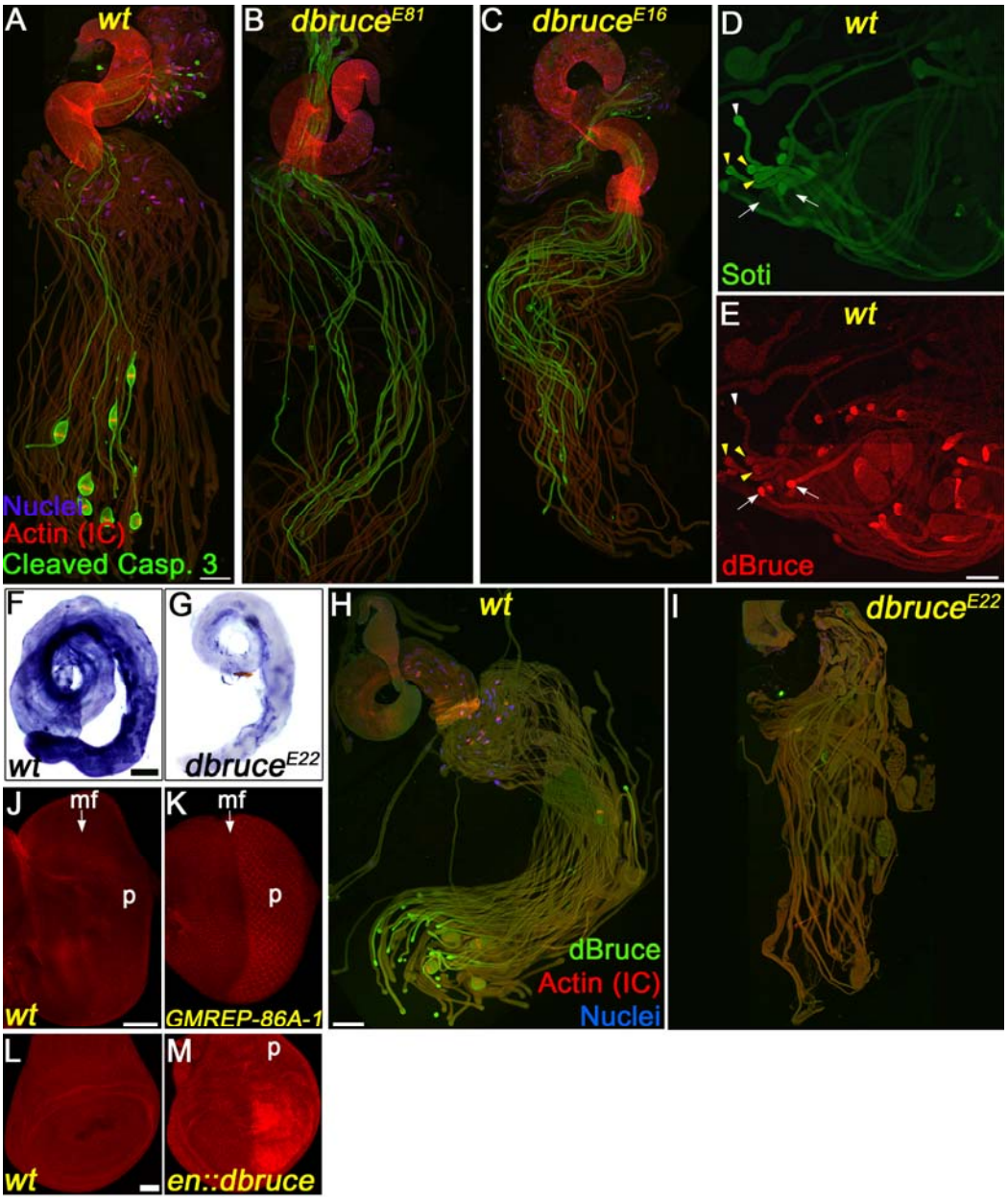


**Figure S5. *dbruce* Mutant Spermatids Display Severe Individualization Defects and dBruce is Expressed in a Gradient of the Same Direction as that of Soti, Albeit at a Different Time, related to Figure 7**

(A-C) Testes from wild-type (A) and two *dbruce* mutant alleles (*dbruce*$^{E81}$; B) and (*dbruce*$^{E16}$; C) were stained to visualize the active effector caspase (anti-cleaved caspase-3 antibody; green), ICs (phalloidin; red), and nuclei (DAPI; blue). Note the large amount of elongated spermatid cysts that express active effector caspase but fail to individualize in the *dbruce* mutants. These spermatids generally maintain high and homogenous levels of active effector caspase throughout their length, as they fail to expel their cytoplasmic content into waste bags. Scale bar, 100 μm.

(D, E) Soti protein is degraded at the time dBruce starts to accumulate. Wild-type spermatids were double-stained to visualize Soti (green) and dBruce (red). (D) Green channel and (E) red channel. A white arrowhead points to elongating spermatid cyst

that only expresses Soti. Yellow arrowheads point to spermatid cysts in which Soti levels start to decline, while dBruce becomes visible at distal tail ends. White arrows indicate more advanced spermatid cysts that readily express the dBruce protein gradient, but show no Soti expression. Scale bar, 100 μm.

(F-M) The anti-dBruce Antibody specifically detects dBruce protein *in vivo*. (F, G) RNA *in situ* hybridization was performed on whole mount testes from wild-type (F) and $dbruce^{E22}$ mutant (G) flies using a specific *dbruce* probe. The $dbruce^{E22}$ is a strong loss-of-function allele of *dbruce*, which was isolated in a genetic screen (for more details about this screen see Arama et al., 2003). Since we could not detect any mutation in the coding region of *dbruce* in this mutant, we postulated that the mutation is in the regulatory region of this gene. Indeed, a dramatic decrease in the level of *dbruce* transcripts is detected in $dbruce^{E22}$ -/- testes (G), compared to the level in wild-type (F). Scale bar, 100 μm.

(H, I) The anti-dBruce antibody readily detects dBruce in wild-type spermatids (H), while a very low dBruce protein is detected in $dbruce^{E22}$ -/- spermatids. Scale bar, 100 μm.

(J, K) Eye-imaginal discs from wild-type flies display low levels of dBruce expression (red) detected by the anti-dBruce antibody (J), whereas elevated levels of expression are detected in flies with the *GMREP-86A-1* transposon insertion (K). This transposon is inserted upstream of the *dbruce* genomic locus and was shown to drive ectopic expression of dBruce posterior (p) to the morphogenetic furrow (mf) via the eye specific enhancer GMR (Vernooy et al., 2002). Scale bar, 50 μm.

(L, M) Whereas no dBruce is detected in wing-imaginal discs of wild-type controls using the anti-dBruce antibody (L), a UAS-dependent transgenic fragment of *dbruce* (encoding for the N-terminus 1,622 a.a. fragment; red) is detected throughout the posterior (p) wing compartment following ectopic expression under the control of the *en-Gal4* driver (M). Scale bar, 50 μm.

## Supplemental Experimental Procedures

### Additional Fly Strains

*dbruce*$^{E81}$ and *dbruce*$^{E22}$ lines were isolated in a genetic screen described in (Arama et al., 2003). The *dbruce*$^{E16}$ and *GMREP-86A-1* lines are described in (Vernooy et al., 2002), the *GMR-Gal4* on the X chromosome in (Hirose et al., 2001), and the *en-Gal4* line in (Ryoo et al., 2004).

### Expression Constructs

The *soti* rescue constructs were generated as follows: a 726 bp fragment of the presumed promoter region and 5' UTR of *soti* (forward primer GGCCAATTGCCATTACAGGCACACAAACAG and reverse primer GCGCAGATCTTCCAACTTACAGGCACATAC with added MfeI and BglII restriction sites, respectively) and a 756 bp fragment of the 3' UTR of *soti* (forward primer GCTGCGGCCGCTTCGCCATAGTTCTCCCATAGA and reverse primer GCTGGTACCACAAGAATGCCGAGGGAGAGAT with added NotI and Acc65I restriction sites, respectively) were PCR amplified from genomic DNA and subcloned in a sequential order into the EcoRI + BglII and NotI + Acc65I sites, respectively, of the pattB vector (a gift from Johannes Bischof). Subsequently, each one of the *soti* ORF forms (*soti*, *soti*$^{3KR}$, *myc-soti* and *myc-soti*$^{3KR}$) with added BamHI and NotI sites were subcloned into the BglII and NotI sites between the *soti* 5' and 3' UTRs within the pattB vector. The intact (*soti*) ORF was amplified by PCR using the BDGP's EST clone GH20124 as a template (forward primer CCAGGATCCATGGACGTACTACACGGACACG and reverse primer AAGCGGCCGCTCAGAACTGACCCCAATGCT). The *soti*$^{3KR}$ form was generated by standard site-directed mutagenesis (forward primer GGACCACCACGTCGGCGGAGGAGACGAAGTTTCTACACTATGACCAGACC CACTCCGCCATGCC and its complimentary reverse primer). To generate the 6x-myc tagged forms (*myc-soti* and *myc-soti*$^{3KR}$), PCR amplified *soti* or *soti*$^{3KR}$ ORF fragments (forward primer CCGGAATTCGGACGTACTACACGGACACG with an added EcoRI site, reverse primer as above) were subcloned into a 6x-myc-containing vector and excised by BamHI + NotI.

To generate the *UAS-klhl10* and *UAS-klhl10*$^{G496R}$ constructs, the ORF of *klhl10* (a 2316 bp fragment) was PCR amplified from BDGP's EST clone AT19737 (forward primer GCCGAATTCATGAGTCGTAATCAAAACG, reverse primer CGCGGTACCCTATGTACGACGACGAATTT, with added EcoRI and Acc65I sites, respectively) and subcloned into the EcoRI + Acc65I sites of the pUASTattB vector (a gift from Johannes Bischof). The mutant *klhl10*$^{G496R}$ fragment that bears a lesion identical to the *klhl10*$^{5}$ mutant was generated by standard site-directed mutagenesis (forward primer CGCATATATGCTACAGGGAGATTTAACGGCCAGGAATG and the complementary reverse primer).

The above transgenic flies were generated using the φC31-mediated site specific transgenesis technique, which allows insertion of transgenes into known sites of the *Drosophila* genome. All the transgenes were inserted into the attP40 site on chromosome 2L (Fish et al., 2007; Bischof et al., 2007).

To generate the *UAS-cullin-3*$_{Testis}$ and *UAS-cullin-3*$_{Testis}^{[-CHD]}$ constructs, the ORF of *cul3*$_{Testis}$ (a 2817 bp fragment) was PCR amplified from the BDGP's EST clone AT07783 (forward primer ATGCAAGGCCGCGATCCCCG and reverse primer TTAGGCCAAGTAGTTGTACA with added *Xho*I and *Nhe*I restriction sites, respectively) and ligated into the *Xho*I and *Xba*I sites within the pUAST vector. The

*cullin-3*$_{Testis}^{[-CHD]}$ construct carries a G2602-to-T transversion that converts glutamic acid (E868) to a stop codon, resulting in catalytically inactive protein which lacks the C-terminal Cullin-homology-domain (CHD). This mutation was generated unintentionally during the PCR amplification.

To generate the *UAS-soti* construct, the ORF of *soti* was PCR amplified from the BDGP's EST clone GH20124 (forward primer CCAGAATTCATGGACGTACTACACGGACACG and reverse primer GTTCGGTACCTCAGAACTGACCCCAATGCTG with added EcoRI and Acc65I sites) and ligated into the EcoRI and Acc65I sites within the pUAST vector.

The *UAS-soti-EGFP* construct was generated as follows: The *soti* ORF was first PCR amplified from BDGP's EST clone GH20124 (forward primer CCAGGATCCATGGACGTACTACACGGACACG and reverse primer GCACCGGTGGGAACTGACCCCAATGCTGTGG with added BamHI and AgeI sites) and ligated into the BglII and AgeI sites of the pEGFP-N1 vector. The resulting *soti-EGFP* fragment was PCR amplified (forward primer CCAGGATCCATGGACGTACTACACGGACACG and reverse primer GCGGCG GCCGCTTTACTTGTACAGC with added BamHI and NotI sites) and ligated into the BglII and NotI sites of the pUASTattB vector.

The *UAS-dbruce* (1-1622), *UAS-dbruce* 'mini-gene', *UAS-HA-dbruce* 'BIR', *UAS-PrA-Klhl10* and *UAS-PrA-GFP* are described in (Arama et al., 2007).

To generate the *UAS-myc-klhl10* construct, *klhl10* ORF was tagged at the N-terminus with a 6xmyc-tag, PCR amplified (forward primer GGAAGCGGCCGCGATCCCATCGATTTAAAGCT and reverse primer GGCCGGTACCCTATGTACGACGACGAATTT with added NotI and Acc65I sites), and ligated into the NotI and Acc65I sites of the pUASTattB vector.

For the *UAS-HA-klhl10* construct, *klhl10* ORF was PCR amplified from BDGP's EST clone AT19737 (forward primer which also contains a single HA-tag AGGGAATTCATGTACCCATACGATGTTCCTGACTATGCGAGTCGTAATCA AAACG and reverse primer CGCGGTACCCTATGTACGACGACGAATTT with added EcoRI and Acc65I sites) and ligated into the EcoRI and Acc65I sites of the pUASTattB vector.

To generate the *UAS-HA-dbruce* 'mini-gene' construct the entire 'mini-gene' fragment was PCR amplified from the *UAS-dbruce* 'mini-gene' plasmid (forward primer which contains a single HA-tag GAGAATTCATGTACCCATACGATGTTCCAGATTACGCTGCCACGGAGCAG CATCACC and reverse primer GGCTCTAGACTATTGCCACATACTGCTCTCG with added EcoRI and XbaI sites) and ligated into the EcoRI and XbaI sites of the pUASTattB vector.

The *pUASt-CD8-GFP*, *pUASTattB-EGFP* and *pAct5-Gal4* constructs were obtained from Ben-Zion Shilo (WIS, Rehovot, Israel).

The *pAct5c-3xFLAG-Ub* was obtained from Gregory C. Rogers (University of Arizona).

The *pUAST-Roc1a* construct was obtained from Robert J. Duronio (University of North Carolina at Chapel Hill).

Transgenic flies were generated by micro-injections into embryos performed by Genetic Services Inc (Sudbury, MA).

**Yeast-Two-Hybrid Screen and Constructs**

Transformation was carried out essentially as described by the Gietz Lab Yeast Transformation Home Page (http://home.cc.umanitoba.ca/~gietz/). Out of ~8.5x10$^6$

clones screened (more than twice the number of independent library clones), 95 clones grew on synthetic complete media lacking all the four nutrients, of which 33 corresponded to *soti*.
The Klhl10 "bait" constructs were generated as follows: a 1,761-bp fragment containing the Klhl10 coding region which lacks the BTB domain (amino acids 188-767) was PCR amplified from the BDGP's EST clone AT19737 (Forward primer CCCGAATTCCGCATACTCACCCCCGAAAA and reverse primer GCCCTGCAGCTATGTACGACGACGAATTT with added EcoRI and PstI sites, respectively), and subcloned in-frame to the GAL4 DNA binding domain using the *Eco*RI and *Pst*I sites of the pGBKT7 vector (Matchmaker, Clontech). The mutated forms of Klhl10 were generated by standard site-directed mutagenesis (forward primers: CCAATGAACATGCAACGCTTTGATGCCAGCGCCTGTAC for S480F, CGCATATATGCTACAGGGAGATTTAACGGCCAGGAATG for G496R, and CGACGATCTCTCATACGAAATGCTATGTAGCCGAAAC for E601K. The reverse primers were complementary to each one of the forward primers).

**Generation of the anti-Soti and anti-dBruce antibodies**
The guinea pig polyclonal anti-Soti antibody was generated as follows: a 464-bp fragment containing the entire *soti* ORF was PCR amplified from BDGP's EST clone GH20124 (forward primer TCGGAATTCGACGTACTACACGGACACGATC and reverse primer CTGGCGGCCGCTCAGAACTGACCCCAATGCTG with added EcoRI and NotI sites, respectively) and ligated in-frame to GST, using the EcoRI and NotI sites of the pGEX-4T-1 vector. The expression plasmid was transformed into BL21/RIL bacteria, followed by 1 hr IPTG induction to express GST-Soti fusion. GST-Soti was purified under native conditions using Glutathione-agarose (Sigma) and used to raise polyclonal antibodies in guinea pigs.
For immunofluorescence experiments, GST-Soti anti-serum was affinity purified using recombinant $His_6$-Soti bound to cyanogen bromide-activated-Sepharose (Sigma). The recombinant $His_6$-Soti was generated as follows: a 461-bp fragment containing the entire *soti* ORF was PCR amplified from BDGP's EST clone GH20124 (forward primer ACGCTCGAGGACGTACTACACGGACACGATC and reverse primer CTGGCGGCCGCTCAGAACTGACCCCAATGCTG with added XhoI and NotI sites, respectively) and ligated in frame to $His_6$ using the XhoI and NotI sites of a derivative plasmid of the pET14b (Novagen). $His_6$-Soti expression was induced by IPTG for 1 hr in BL21/RIL bacteria, followed by nickel chromatography purification under denaturing conditions using Ni-NTA His-Bind Resin (Qiagen).
The dBruce antiserum was generated as follows: a 1931-bp fragment containing the N-terminal 637 amino acids of dBruce was PCR amplified from the BDGP's EST clone LD31268 (forward primer GGCCTCGAGGCCACGGAGCAGCATCACCA and reverse primer: GGCGCGGCCGCCTACAGCTTATTAATCTCGTTGC with added XhoI and NotI sites, respectively) and ligated in frame to $His_6$ using the XhoI and NotI sites of a derivative plasmid of the pET14b (Novagen). Expression of the $His_6$-dBruce protein fragment was induced by IPTG for 1.5 hr in BL21/RIL bacteria. The $His_6$-dBruce fragment was purified by nickel affinity chromatography under denaturing conditions using Ni-NTA His-Bind Resin (Qiagen) and was used to raise polyclonal antibodies in rabbits (the Antibody Unit at the Weizmann Institute, Rehovot).

**Isolation of Genomic DNA and PCR**

Genomic DNA was isolated from ~30 adult flies using the High Pure PCR Template Preparation Kit (Roche). 100 ng or 200 ng of genomic DNA were used for PCR amplification for subsequent sequencing or cloning, respectively. PCR reactions were carried out using PfuUltra II Fusion HS DNA Polymerase (Stratagene), according to the manufacturer's instructions.

**Immunohistochemistry of Testis Sections**

Testes of adult young males (0-2 days old) were fixed in 4% paraformaldehyde in PBS for 20 minutes, washed 3 times in PBS, transferred to 30% sucrose, incubated overnight at 4$^{o}$C and embedded in OCT. Sections were cut (8 μm thick) and mounted on Superfrost Plus slides. The slides were dried for 30 minutes at room temperature. Following blocking for 1 hour in PHT (0.1% Triton, 1% Goat Serum in PBS), sections were incubated at 4$^{o}$C in a humid chamber with the appropriate diluted antibodies in a blocking solution (see the Immunofluorescence Staining section for details). The sections were washed 3 times with PHT, incubated with the secondary antibody diluted in PHT 1:250 for 2 hours at room temperature in a humid chamber; washed 3 times in PBS and mounted in Vectashield medium (Vector laboratories).

**RNA in Situ Hybridization**

RNA in situ hybridization on testes was performed as described in (White-Cooper, 2004). The *soti* probe was generated as follows: a 605-bp fragment that contains parts of *soti* ORF and 3' UTR sequences was PCR amplified from genomic DNA (forward primer GCGCGGCCGCAATGGTATGGGTCTGCCACAG and reverse primer CGGGTACCGGTGCTGCAAGAGGGAGTAG with added NotI and Acc65I sites, respectively) and ligated into the NotI and Acc65I sites of the skII vector.

The *dbruce* probe was generated as follows: a 680-bp fragment that contains parts of *dbruce* ORF and 3' UTR sequences was PCR amplified (forward primer GCGCGGCCGCGGCCAGTCGCACTATATCGT and reverse primer CGGGTACCGTATGTGTGCACGCCCTCTT with added NotI and Acc65I sites, respectively) from the T1A-ClaI cDNA clone (Arama et al., 2007), and ligated into the NotI and Acc65I sites of the skII vector.

## Supplemental References


Arama,E., Agapite,J., and Steller,H. (2003). Caspase activity and a specific cytochrome C are required for sperm differentiation in Drosophila. Dev. Cell *4*, 687-697.

Arama,E., Bader,M., Rieckhof,G.E., and Steller,H. (2007). A Ubiquitin Ligase Complex Regulates Caspase Activation During Sperm Differentiation in Drosophila. PLoS Biol *5*, e251.

Bischof,J., Maeda,R.K., Hediger,M., Karch,F., and Basler,K. (2007). An optimized transgenesis system for Drosophila using germ-line-specific phiC31 integrases. Proc. Natl. Acad. Sci. U. S. A *104*, 3312-3317.

Fish,M.P., Groth,A.C., Calos,M.P., and Nusse,R. (2007). Creating transgenic Drosophila by microinjecting the site-specific phiC31 integrase mRNA and a transgene-containing donor plasmid. Nat. Protoc. *2*, 2325-2331.

Hirose,F., Ohshima,N., Shiraki,M., Inoue,Y.H., Taguchi,O., Nishi,Y., Matsukage,A., and Yamaguchi,M. (2001). Ectopic expression of DREF induces DNA synthesis, apoptosis, and unusual morphogenesis in the Drosophila eye imaginal disc: possible interaction with Polycomb and trithorax group proteins. Mol. Cell Biol. *21*, 7231-7242.

Ryoo,H.D., Gorenc,T., and Steller,H. (2004). Apoptotic cells can induce compensatory cell proliferation through the JNK and the Wingless signaling pathways. Dev. Cell *7*, 491-501.

Vernooy,S.Y., Chow,V., Su,J., Verbrugghe,K., Yang,J., Cole,S., Olson,M.R., and Hay,B.A. (2002). Drosophila Bruce can potently suppress Rpr- and Grim-dependent but not Hid-dependent cell death. Curr. Biol. *12*, 1164-1168.

White-Cooper,H. (2004). Spermatogenesis: analysis of meiosis and morphogenesis. Methods Mol. Biol. *247*, 45-75.